NATIONAL ADVISORY COMMITTEE FOR AERONAUTICS

TECHNICAL NOTE

No. 1199

CHARTS OF PRESSURE RISE OBTAINABLE WITH AIRFOIL-TYPE AXIAL-FLOW COOLING FANS

By A. Kahane

Langley Memorial Aeronautical Laboratory
Langley Field, Va.

Washington
March 1947

NATIONAL ADVISORY COMMITTEE FOR AERONAUTICS

TECHNICAL NOTE NO. 1199

CHARTS OF PRESSURE RISE OBTAINABLE WITH AIRFOIL-TYPE AXIAL-FLOW COOLING FANS

By A. Kahane

SUMMARY

Charts are presented to show the pressure rise that is obtainable in an engine-cooling installation with a typical airfoil-type propeller-speed fan. The charts cover fans of the stator-rotor, rotor-stator, and rotor alone configurations, with blades incorporating both the highly cambered 65-series blower-blade sections and the conventional low-cambered airfoil sections. The effects of operation of a geared fan with rotational speeds limited by compressibility considerations and the effects of initial rotational inflow are indicated. Use of the charts to predict the pressure rise obtainable with any fan of the types considered is illustrated in a sample calculation.

The cooling pressure rise obtainable with a propeller-speed fan at low altitudes is shown to be large and may be sufficient for most installations. At high altitudes the pressure rise is small. Of the three configurations operating as propeller-speed fans, the stator-rotor arrangement is shown to furnish the highest pressure rise. The pressure rise obtainable at a given flight velocity increases with increasing fan-velocity ratio. A geared fan is shown to have a possible pressure rise of approximately 95 inches of water at sea level and 18 inches of water at 40,000 feet when the mean relative Mach number at the tip is 0.8.

Rotational inflow in either direction is shown to cause an increase in pressure rise directly across the fan with the stator-rotor arrangement. The pressure rise obtainable with a rotor alone is decreased by rotational inflow in the direction of fan rotation and increased by inflow in the opposite direction. The pressure rise obtainable with a rotor-stator may be either increased

or decreased by inflow in the direction of fan rotation and is increased by inflow in the opposite direction.

INTRODUCTION

Higher pressure rise than was previously thought possible is now obtainable with axial-flow cooling fans. In a recent investigation (reference 1) of a family of NACA 65-series blower-blade sections tested in cascade, it was shown that values of the product of solidity σ times section lift coefficient c_l as high as 1.3 may be obtained with highly cambered airfoils. Previously, a value of $c_l = 0.7$, for solidities of about unity, has been considered approximately the maximum for fan design (reference 2), with the low-cambered R.A.F. 6 type of airfoil section in general use.

The present paper contains charts showing the pressure rise that is obtainable in an engine-cooling installation with a typical airfoil-type propeller-speed fan both with highly cambered 65-series blower-blade sections and with conventional low-cambered sections. These charts have been prepared for single-stage fans having a rotor alone, a stator following a rotor, and a rotor following a stator. Additional charts have been prepared to indicate the effects of operation of a configuration for which the rotational speeds are limited only by compressibility effects (such as a geared fan) and the effects of rotational inflow, as caused by a tractor propeller. Material has been included to make the charts applicable to the determination of pressure rise obtainable with fans of any given dimension at any operating condition.

SYMBOLS

a	velocity of sound, feet per second
A	area, square feet
b	blade section chord, feet
B	number of blades

c_l section lift coefficient

d fan diameter at a section, feet

K_1 fan performance coefficient $\left(\frac{3}{d}\frac{1600}{n}\frac{V_f}{V_o}\right)$

K_2 fan performance coefficient $\left(\left(\frac{3}{d}\frac{1600}{n}\right)^2 = \left(\frac{K_1}{V_f/V_o}\right)^2\right)$

M Mach number (V/a)

n rotational speed, rpm (except when otherwise noted)

N rotation parameter $(\omega r/V_f)$

Δp fan static-pressure rise, inches of water

q dynamic pressure, inches of water $\left(\frac{\rho V^2}{2}\right)$

q_f axial dynamic pressure at fan, inches of water $\left(\frac{\rho_f V_f^2}{2}\right)$

r radius at a section, feet

R outside radius of fan, feet

u absolute tangential velocity, feet per second

V absolute velocity, feet per second

V_f axial velocity at fan, feet per second

W mean relative velocity at rotor, feet per second

x radius ratio (r/R)

β stagger angle; angle between relative entering air to rotor and fan axis, degrees

δ angle of initial rotational inflow to fan, degrees $\left(\tan^{-1}\frac{u_p}{V_f}\right)$

θ turning angle, degrees

γ ratio of specific heats (1.4 for air)

η efficiency $\left(\frac{\Delta p_{actual}}{\Delta p_i}\right)$

ρ mass density of air, slugs per cubic foot

σ solidity $\left(\frac{Bb}{2\pi r}\right)$

ω angular velocity of rotating blades, radians per second

Subscripts:

f at fan

h hub

i ideal

o free stream

0 zero rotational inflow

out outside

p behind propeller

r rotor

r-s rotor-stator

s stator

s-r stator-rotor

W mean relative velocity

Primes on symbols indicate condition of initial rotational inflow.

CONSIDERATIONS AFFECTING PRESSURE RISE

Formulas for Pressure Rise of a Fan Element

A detailed discussion of axial-flow-fan theory and design may be found in reference 2, in which equations are derived for the ideal pressure-rise coefficient $\Delta p_i/q_f$ of a fan blade element (assumed independent of its neighboring elements) in terms of the rotor σc_l and N of the element. The ideal pressure rise is defined as the pressure rise that would occur in a frictionless fluid. These equations are derived on the basis of incompressible flow for single-stage fans of configurations having (1) the stator upstream of rotor, (2) the rotor upstream of stator, and (3) the rotor alone. These configurations are designated stator-rotor, rotor-stator, and rotor, respectively. The ideal pressure rise, expressed in coefficient form, for each of these configurations is given in reference 2 as:

Stator-rotor:

$$\left(\frac{\Delta p_i}{q_f}\right)_{s-r} = \frac{1 + \sqrt{1 + \left(\frac{1}{N^2} + 1\right)\left(\frac{16}{\sigma^2 {c_l}^2} - 1\right)}}{\frac{1}{4N^2}\left(\frac{16}{\sigma^2 {c_l}^2} - 1\right)} \qquad (1)$$

Rotor-stator:

$$\left(\frac{\Delta p_i}{q_f}\right)_{r-s} = \frac{-1 + \sqrt{1 + \left(\frac{1}{N^2} + 1\right)\left(\frac{16}{\sigma^2 {c_l}^2} - 1\right)}}{\frac{1}{4N^2}\left(\frac{16}{\sigma^2 {c_l}^2} - 1\right)} \qquad (2)$$

Rotor:

$$\left(\frac{\Delta p_i}{q_f}\right)_r = \left(\frac{\Delta p_i}{q_f}\right)_{r-s} - \left(\frac{1}{4N^2}\right)\left(\frac{\Delta p_i}{q_f}\right)^2_{r-s} \qquad (3)$$

The velocity diagrams corresponding to each arrangement are presented in figure 1.

The stator-rotor and rotor-stator equations were derived on the assumption that no rotational velocity exists upstream or downstream of the stage and, therefore, the ideal static-pressure rise is equivalent to the ideal total-pressure rise. The ideal total-pressure rise for the rotor alone is equal to that of a similar rotor-stator, inasmuch as no change of total energy takes place in the flow through the stator.

The ideal pressure-rise coefficient obtained from reference 2 is plotted as a function of $\bar{N}$ for values of σc_l of 0.7, 1.0, and 1.3 in figure 2.

Formulas for Average Pressure Rise in the Annulus

The design criterion for the constant-velocity fan (that is, a fan through which the axial velocity of the flow remains uniform), also known as the free-vortex fan, is that the circulation around each blade element is constant radially. For this type of fan, the greatest value of σc_l occurs at the blade hub and for the rotor-stator and stator-rotor configurations the ideal pressure rise is constant radially at the design point. If, therefore, $(\sigma c_l)_h$ and N_h are known, the average ideal pressure rise for the stator-rotor and rotor-stator may be determined from figure 2.

In the determination of the average ideal pressure rise for the rotor alone, equation (3) and the rotational static-pressure loss averaged over the fan disk area may be used. The average loss is

$$\text{Average rotational loss} = \frac{1}{A}\int^{A} \frac{1}{4N^2}\left(\frac{\Delta p_i}{q_f}\right)^2_{r\text{-}s} dA$$

$$= \frac{\left(\frac{\Delta p_i}{q_f}\right)^2_{r\text{-}s}}{2N_{out}^2\left(1 - x_h^2\right)} \log \frac{1.0}{x_h}$$

Thus, the average ideal static-pressure rise for the rotor is

$$\left(\frac{\Delta p_i}{q_f}\right)_{r_{av}} = \left(\frac{\Delta p_i}{q_f}\right)_{r\text{-}s} - \frac{\left(\frac{\Delta p_i}{q_f}\right)^2_{r\text{-}s}}{2N_{out}^2\left(1 - x_h^2\right)} \log \frac{1.0}{x_h} \quad (4)$$

In order to determine the actual pressure rise, the various fan losses such as profile drag, tip clearance, and hub boundary losses should be subtracted from the average ideal pressure rise. For the purposes of estimation, it is sufficient to multiply the ideal pressure rise by an estimated efficiency to find the actual pressure rise; thus

$$\Delta p_{actual} = \eta \Delta p_i$$

For a cooling-fan installation with the fan operating at its design point with uniform entry-flow conditions, a value of $\eta = 0.80$ may be considered representative. When the entry flow is nonuniform, as in a cowling installation at a high angle of attack, the efficiency may be considerably less than 0.80.

Maximum Obtainable Design σc_l and Pressure Rise

The conclusion was reached in reference 2, after a survey of the limited cascade data available, that the maximum design c_l of a rotor airfoil in cascade was about 0.7. The airfoils tested in cascade up to that time were low-cambered sections of the R.A.F. 6 type generally used in

axial fans. Since then, the cascade tests reported in reference 1 have been conducted, and the more highly-cambered low-drag sections tested were found to produce much higher lift coefficients. The data also show that c_l alone cannot be used as a criterion, since the maximum value of c_l suitable for design will vary with solidity and stagger.

In the investigation of reference 1, the NACA 65-series blower-blade sections ranging in camber from free-air design lift coefficients of 0 to 1.8 were tested at solidities of 1.0 and 1.5 and at stagger angles of 45° and 60°. The design point of a section was defined as the point at which a reasonably flat pressure distribution existed on the suction surface of the airfoil. The results indicate that a design value of σc_l of 1.3 can be obtained for stagger angles up to 60°. Unpublished results from the investigation of reference 1 indicated that values of σc_l greater than 1.3 can be obtained at stagger angles equal to and less than 45°. In the calculations presented herein, however, it will be conservatively assumed that the maximum obtainable value of σc_l for a rotor is 1.3 for stagger angles up to 60°. Although the tests were not conducted at stagger angles greater than 60°, the trends shown by the results indicate that the maximum design σc_l will be less than 1.3 in this region. In the calculations of the c_l obtained at maximum pressure rise from fan test data (reference 3), the maximum c_l was also found to drop in the high stagger range. In this range of stagger angle the pressure rise is high, and the stall of the blades is accelerated by the thickening and separation of the boundary layer because of the steep pressure gradient. For stagger angles greater than 60°, the criterion for blade stall may therefore be expected to be the pressure rise relative to the mean relative dynamic pressure at the blade $\Delta p/q_W$ $\left(\text{where } q_W = \frac{\rho}{2} W^2\right)$ rather than the blade-loading factor σc_l.

The value of $\Delta p_1/q_W$ for $\sigma c_l = 1.3$ at 60° stagger is 0.98 and, in the absence of more complete experimental information, it will be assumed herein that for stagger angles greater than 60°, this value is a maximum for design purposes. The maximum σc_l obtainable for design

was calculated following this assumption and values of maximum σc_l are plotted in figure 3 as a function of stagger angle. The equation for stagger angle for the rotor-stator and rotor is

$$\tan \beta = N$$

and for the stator-rotor is

$$\tan \beta = N + \frac{1}{2N}\left(\frac{\Delta p_1}{q_f}\right)_{s-r}$$

From these equations the maximum obtainable σc_l was related to the rotation parameter N as shown in figure 4. The ideal pressure rise for stagger angles greater than 60°, based on the maximum σc_l obtainable as determined from figure 4, was calculated according to equations (1) to (3) and is presented as a function of N in figure 5.

The foregoing criterion for the maximum values of σc_l obtainable will be applied only to the rotor herein. It is assumed in the charts of figure 6 that stators can be designed to operate properly with a rotor loaded to the maximum values of σc_l obtainable. In the stator-rotor and rotor-stator configurations, the value of σc_l required for the stator is larger than that of the rotor when the mean velocity of the rotor is greater than that of the stator. Tests of entrance vanes in cascade (reference 4) indicate that because of the pressure drop, axially entering air can be deflected efficiently up to angles of 80°. Thus, no difficulty would be encountered in the design of the stators for the stator-rotor configuration. In the rotor-stator configuration, the stator must act in a pressure-rise condition similar to that of the rotor and the same criterion for maximum values of σc_l obtainable would apply. As mentioned previously, unpublished data of cascade tests indicate that values of σc_l greater than 1.3 may be obtained at stagger angles equal to and less than 45°. For a rotor having a stagger angle of 60° and operating at $\sigma c_l = 1.3$, the stagger angle of the stator is about 46°. For this condition, the value of σc_l required for the stator is about 1.7. The unpublished cascade tests indicate that this value of σc_l may be obtained. For rotor stagger angles up to 60°,

therefore, a single-stage stator may be utilized with the rotor-stator configuration. When the rotor stagger angle is larger than 60°, the stagger angle of the stator is larger than 46° and the stator is required to supply much larger values of σc_l than the rotor. Thus, long diffuser-like stators or a two-stage stator may be required in this operating range to return the flow completely to the axial direction. Little data are available for such stators and it is possible that difficulty with the boundary layers at the walls may cause high losses. It may be noted, however, that a large part of the static-pressure rise obtainable from the rotating stream behind a rotor may be realized even though the air leaving the stator is 10° or 20° to the axial direction.

PRESSURE RISE OBTAINABLE WITH COOLING FANS

With Axial Inflow

Propeller-speed fan.- Charts showing the pressure rise that can be attained with a typical propeller-speed fan having the highly cambered NACA 65-series blower-blade sections are presented in figure 6. These curves are based on the maximum σc_l relationship shown in figure 3. The charts were computed to indicate the ideal pressure-rise coefficient $\frac{\rho_o}{\rho_f}\frac{\Delta p_i}{q_o}$ at a fan section diameter of 3 feet and a fan rotational speed of 1600 rpm. For the free-vortex type of fan discussed in the previous section the charts give the average pressure rise for stator-rotor and rotor-stator fans of 3-foot hub diameter and 1600-rpm rotational speed. The chart for the rotor alone (fig. 6(c)) does not give values of the average pressure rise, since no outside diameter has been designated, but indicates the pressure rise to be expected at the hub of a rotor of 3-foot hub diameter operating at 1600 rpm. The average rotor pressure rise, if desired, may be found from equation (4). The ordinates and curves of the charts have two designations and for the typical propeller-speed fan the first designation is used. The second designation generalizes the charts with respect to the determination of pressure rise for fans of any diameter and rotational speed and is discussed subsequently in the section "Fan Charts and Illustrative Example." The charts (fig. 6) show the ideal pressure-rise coefficient based on free-stream dynamic pressure that may be obtained for several

fan-velocity ratios V_f/V_o through a flight velocity range of 120 to 400 miles per hour. The pressure-rise coefficient is shown to increase with increasing fan-velocity ratio for the rotor-stator and stator-rotor. For the rotor the pressure rise increases with fan-velocity ratio in the low flight-velocity range but decreases in the high flight-velocity range and actually is negative at very high fan-velocity ratios. This phenomenon results because, at low stagger angles, the blade operating at a high σc_l turns the air through such a large angle as to cause most of the energy input to be converted to rotational energy rather than to static-pressure rise.

Charts showing the ideal pressure-rise coefficient $\frac{\rho_o}{\rho_f}\frac{\Delta p_i}{q_o}$ that may be obtained for a typical propeller-speed fan of the previously mentioned dimensions with blades of low-cambered sections $(\sigma c_l = 0.7)$ are shown in figure 7. At a given flight velocity, the pressure rise is noted to increase with fan-velocity ratio for the stator-rotor and rotor-stator, and also for the rotor alone over its practical operating range.

The ideal pressure rise in inches of water that may be obtained by the typical propeller-speed fan at several altitudes is shown in figure 8 for the fan velocity ratio $\frac{V_f}{V_o} = 0.6$. Army standard air density was used in these calculations. The figure shows that for a given fan-velocity ratio the value of obtainable pressure rise increases with increasing flight velocity, and that the highly cambered sections (maximum obtainable σc_l) furnish considerably higher pressure rise than the conventional low-cambered sections $(\sigma c_l = 0.7)$. It is also evident that the greatest pressure rise is obtained with the stator-rotor configuration, and that this type of fan should be used when the rotational speed is limited, if the highest pressure rise obtainable is desired. The propeller-speed fan appears to provide sufficient cooling at low altitudes. At high altitudes, the pressure rise obtainable is small.

Geared fan.- The effect on ideal pressure-rise coefficient of changing the rotational speed is shown in

figure 9, wherein it is evident that large increases in pressure rise may be obtained by gearing the fan.

The maximum fan pressure rise that may be achieved by rotating the fan at high speeds is limited by compressibility considerations. In reference 2 a method is given of solving for the maximum pressure rise and rotational speed of a fan of known dimensions, quantity flow, and σc_l at the hub, the mean relative velocity at the tip being set equal to some fraction of the velocity of sound. The results presented in reference 2 also proved that, for fans of hub-tip radius ratio x_h greater than 0.707, the greatest pressure rise may be obtained from the rotor-stator configuration.

The NACA 65-series blower-blade sections are now being investigated in high-speed flow. Preliminary indications are that the critical mean relative Mach number W/a will be between 0.6 and 0.8, depending upon the section camber and loading.

Calculations were made by the method of reference 2 of the maximum ideal pressure rise of a rotor-stator of $x_h = 0.75$, $(\sigma c_l)_h = 1.0$, and mean relative Mach number $\frac{W}{a} = 0.6$ and 0.8. The fan was also assumed to be in an inlet. The density ratio ρ_f/ρ_o was calculated from the equation

$$\frac{\rho_f}{\rho_o} = \left\{ \left[\frac{\gamma - 1}{2} M_o^2 \left[1 - \left(\frac{V_f}{V_o} \right)^2 \right] + 1 \right]^{\frac{1}{\gamma - 1}} \right. \qquad (5)$$

which was derived from Bernoulli's equation for a compressible fluid. (See reference 5.) The calculations were made for a flight velocity range of 120 to 400 miles per hour, for altitudes from sea level to 40,000 feet, and for fan-velocity ratios from 0.2 to 1.0. The results showed that the pressure rise obtainable and the maximum tip speed at a given W/a varied only 5 percent through the calculated $\frac{V_f}{V_o}$-range at any altitude and flight speed. In figure 10(a) is shown the variation of maximum ideal pressure-rise coefficient with flight velocity and

altitude for $\frac{V_f}{V_o} = 0.6$, which may be considered typical for values of $\frac{W}{a} = 0.6$ and 0.8. In figure 10(b) are values of maximum tip speed (in terms of nd_{out} for convenience) required to give the maximum pressure rise for $\frac{V_f}{V_o} = 0.6$. The maximum ideal pressure rise in inches of water, computed by using Army standard air, is presented in figure 10(c), and the pressure rise at any altitude is shown to be almost constant over the flight-velocity range at a given value of mean relative Mach number. The maximum ideal pressure rise is shown to be approximately 95 inches of water at sea level and 18 inches of water at 40,000 feet in Army standard air for a mean relative Mach number at the tip of 0.8. Figure 10 may be used to determine quickly whether a single-stage fan can furnish a required pressure rise. For example, at an altitude of 30,000 feet in Army standard air and at a flight velocity of 300 miles per hour, a rotor-stator of 3.5-foot outside diameter, with a value of $\frac{W}{a} = 0.8$ at the tip, can supply a maximum ideal pressure rise of about 27 inches of water, at a rotational speed of approximately 4700 rpm.

With Rotational Inflow

General remarks.- When the inlet to the fan is downstream of the propeller, the resulting rotational inflow may affect appreciably changes in the ideal pressure rise and blade-angle setting for any design value of σc_l. Scanty experimental evidence available (British) indicates that the inflow angle δ, resulting from an initial rotational velocity u_p, where

$$\delta = \tan^{-1} \frac{u_p}{V_f}$$

may be as large as 45°. Most of the rotational inflow is probably caused by the rotating boundary layer on the spinner and the interference at the blade root and spinner juncture; therefore, theoretical prediction does not

appear feasible. The analysis treats only the change in static-pressure rise from immediately upstream to immediately downstream of the fan. In estimating the total pressure available for cooling, the total energy of the flow directly behind the propeller must be known. Values of δ and u_p are defined as positive when the inflow rotation is in the same direction as the fan rotation and as negative when the inflow rotation is in the opposite direction to the fan rotation. Use of the charts to estimate rotational inflow effects requires that the value of δ be known or assumed.

Effect of initial rotational inflow on stator-rotor.- Initial rotational inflow increases the ideal pressure rise obtainable directly across the stator-rotor configuration. In this configuration a pressure drop is experienced through the stator, and the initial rotation decreases the pressure drop. The increase of pressure-rise coefficient is derived in appendix A as

$$\frac{\Delta p_1' - \Delta p_1}{q_0} = \frac{\rho_f}{\rho_0}\left(\frac{1}{\cos^2\delta} - 1\right)\left(\frac{V_f}{V_0}\right)^2 \qquad (6)$$

Equation (6) is plotted in figure 11. Significant increases in ideal static pressure rise are seen to be obtainable at high angles of inflow and the higher fan-velocity ratios.

Effect of initial rotational inflow on rotor-stator and rotor pressure rise.- The effect of rotational inflow on the rotor and rotor-stator ideal pressure rise at a fan blade element is shown in figure 12 for inflow rotational direction the same as the fan rotation and in figure 13 for inflow rotational direction opposite to the fan rotation. The effect is presented as the ratio of the change of pressure rise due to rotational inflow to the pressure rise with zero rotational inflow. The curves are plotted for constant values of stagger β_0 of the fan, that is, the stagger angle for zero rotational inflow, where

$$\beta_0 = \tan^{-1} N$$

for constant values of σc_l equal to 0.7, 1.0, and 1.3. It is assumed in these curves that the original σc_l is obtained by changing the fan blade-element angle and that the stator element of the rotor-stator is reset to remove all the rotation from the final stream. The method of calculating the curves is presented in appendix B.

For the rotor alone, inflow rotation in the same direction as fan rotation decreases the obtainable pressure rise and inflow rotation in the opposite direction increases the obtainable pressure rise.

For the rotor-stator, inflow in the direction opposite to fan rotation also increases the obtainable pressure rise. With inflow in the same direction as the fan rotation, a decrease or increase of obtainable pressure rise may be realized by the rotor-stator, depending on the region of fan operation. An increase takes place when the increase of rotational energy behind the rotor is greater than the rotor static-pressure-rise decrease caused by decreasing the stagger.

Because a value of $\sigma c_l = 1.3$ is not obtainable at stagger angles greater than 60°, curves showing the effect of initial rotational inflow on the rotor-stator and rotor ideal pressure rise for maximum obtainable σc_l, as defined in figure 4, are presented in figures 14 and 15.

FAN CHARTS AND ILLUSTRATIVE EXAMPLE

Charts for Determining Pressure-Rise Coefficient

The curves of figures 6 and 7, with a few modifications in notation, may be used to determine quickly the maximum obtainable ideal pressure rise (based on the σc_l relation of fig. 3) or the ideal pressure rise obtainable with a low cambered blade $(\sigma c_l = 0.7)$ of constant-velocity fans of given hub diameter, rotational speed, and fan-velocity ratio V_f/V_o, in the flight-velocity range between 120 and 400 miles per hour. In order to make the charts applicable to any fan the lines of constant fan-velocity are designated K_1, where

$$K_1 = \frac{3}{d} \frac{1600}{n} \frac{V_f}{V_o}$$

The ordinate of figures 6 and 7 then becomes

$$\frac{\rho_o}{\rho_f} K_2 \frac{\Delta p_i}{q_o}$$

where

$$K_2 = \left(\frac{3}{d} \times \frac{160p}{n} \right)^2$$

$$= \left(\frac{K_1}{V_f / V_o} \right)^2$$

The derivation of the coefficients K_1 and K_2 is presented in appendix C. The use of the curves is facilitated by charts for determining K_1 and $\frac{\Delta p_i}{q_o}$ from $K_2 \frac{\Delta p_i}{q_o}$, which are presented in figures 16 and 17. Thus, in order to find the maximum pressure-rise coefficient obtainable at a flight velocity of 300 miles per hour from a stator-rotor of 2-foot hub diameter, 3600-rpm rotational speed, and $\frac{V_f}{V_o} = 0.4$, $K_1 = 0.27$ is first determined from figure 16. Next, $\frac{\rho_o}{\rho_f} K_2 \frac{\Delta p_i}{q_o} = 0.50$ is obtained in figure 6(a), and finally from figure 17(a) it is determined that $\frac{\rho_o}{\rho_f} \frac{\Delta p_i}{q_o} = 1.14$.

In order to facilitate the determination of the effect of rotational inflow for rotor-stator and rotor-alone configurations, a plot of β_0 as a function of K_1 and flight velocity is presented in figure 18.

Illustrative Example

The discussion of the previous sections will be illustrated by the estimation of fan performance for an airplane cruising at 220 miles per hour at an altitude of 35,000 feet. A fan static-pressure rise of 12 inches of water is assumed to be required for cooling and in the example, the following values are determined:

(1) the maximum pressure rise obtainable with propeller-speed fans of the stator-rotor, rotor-stator, and rotor configurations

(2) the rotational speed necessary for each fan configuration in order to supply the required pressure rise

The estimations are first made for zero initial rotational inflow; the effect of an inflow of 20° on the pressure rise at the hub section is then determined. The assumption is made that the propeller-speed-fan rotation is in the same direction as the propeller rotation, whereas the geared-fan rotation is opposite to the propeller rotation.

The following data, based on an actual cooling-installation, were assumed:

Altitude (Army standard air), feet	35,000
Atmospheric density, ρ_o, slug per cubic foot	0.000670
Flight velocity, mph	220
Flight Mach number, M_o	0.32
Propeller-speed-fan rotational speed, rpm	1125
Fan hub diameter, d_h, feet	2.30
Fan-velocity ratio, V_f/V_o	0.60
Propeller rotational inflow, δ, degrees	20
Required fan pressure rise, Δp, inches water	12
Fan efficiency, η	0.80
Required ideal fan pressure-rise coefficient, $\frac{\Delta p_i}{q_o}$	2.24

The steps taken in the calculation are presented in table I and the results of the calculations are as follows:

	Stator-rotor	Rotor-stator	Rotor
Propeller-speed fan			
$\frac{\Delta p_i}{q_o}$ for $\delta = 0^\circ$	0.52	0.36	0.18
$\frac{\Delta p_i}{q_o}$ for $\delta = 20^\circ$	.56	.38	.01
Geared fan			
Fan speed (rpm) for $\delta = 0^\circ$, $\frac{\Delta p_i}{q_o} = 2.24$	3180	4040	4730
$\frac{\Delta p_i}{q_o}$ for $\delta = -20^\circ$	2.28	2.49	2.80

The propeller-speed fan does not supply sufficient pressure rise for cooling and a geared fan is required.

CONCLUSIONS

An analysis has been presented of the pressure rise obtainable with single-stage airfoil-type cooling fans utilizing highly cambered 65-series blower-blade sections. The fan arrangements considered were a stator-rotor, a rotor-stator, and a rotor alone. Several conclusions of importance in the selection of cooling fans may be drawn, as follows:

1. The cooling pressure rise obtainable with a propeller-speed fan is large at low altitudes, and may be sufficient for most installations. At high altitude, the obtainable pressure rise is small. Of the three fan configurations operating as propeller-speed fans, the

highest pressure rises may be obtained with the stator-rotor arrangement.

2. The pressure rise obtainable with a propeller-speed fan increases with increasing fan-velocity ratio at a given flight velocity.

3. The pressure rise obtainable with a fan of which the rotational speed is limited by compressibility effects is almost independent of fan-velocity ratio and flight velocity. The maximum ideal pressure rise is approximately 95 inches of water at sea level and 18 inches at 40,000 feet, in Army standard air for a mean relative Mach number at the tip equal to 0.8.

4. With the fan blades adjusted for satisfactory operation in rotational inflow, the pressure rise obtainable directly across stator-rotor will be increased by rotational inflow in a direction either the same as or opposite to the fan rotation. The pressure rise obtainable with a rotor alone will be decreased by rotational inflow in the direction of fan rotation, and increased by inflow in the opposite direction. The pressure rise obtainable with a rotor-stator may be either increased or decreased, depending on the operating region, by inflow in the direction of the fan rotation and will be increased by inflow rotation in the opposite direction.

Langley Memorial Aeronautical Laboratory
National Advisory Committee for Aeronautics
Langley Field, Va., January 16, 1946

APPENDIX A

DERIVATION OF THE EFFECT OF INITIAL ROTATIONAL INFLOW ON STATOR-ROTOR PRESSURE RISE

For the stator-rotor configuration (see fig. 1), the ideal pressure drop through the stator at $\delta = 0^\circ$ may be expressed by use of Bernoulli's equation as

$$\Delta p_{i_s} = \frac{\rho}{2}\left(V_f^2 - V_1^2\right)$$

When an initial rotation exists upstream of the stator, the pressure drop is

$$\Delta p_{i_s}' = \frac{\rho}{2}\left[\left(\frac{V_f}{\cos \delta}\right)^2 - V_1^2\right]$$

Inasmuch as the rotational inflow only affects the pressure rise through the stator, the increase realized in ideal pressure rise for the stage because of initial rotation is, in coefficient form,

$$\frac{\Delta p_i' - \Delta p_i}{q_f} = \frac{1}{\cos^2 \delta} - 1$$

or, in terms of free-stream dynamic pressure,

$$\frac{\Delta p_i' - \Delta p_i}{q_o} = \frac{\rho_f}{\rho_o}\left(\frac{1}{\cos^2 \delta} - 1\right)\left(\frac{V_f}{V_o}\right)^2 \qquad (6)$$

APPENDIX B

METHOD OF CALCULATING EFFECT OF INITIAL ROTATIONAL INFLOW ON ROTOR-STATOR AND ROTOR PRESSURE RISE

The effect of initial rotational inflow on the ideal pressure rise of the rotor-stator and rotor configurations was determined in the following manner. The rotor may be considered a device that turns the air through an angle θ. (See fig. 1.) The relation between σc_l, the stagger angle β, and the turning angle θ is, if drag is neglected,

$$\sigma c_l = \frac{2\left[\tan \beta - \tan (\beta - \theta)\right]}{\sqrt{1 + \frac{1}{4}\left[\tan \beta + \tan (\beta - \theta)\right]^2}}$$

A plot of β against θ for constant values of σc_l equal to 0.7, 1.0, and 1.3 as determined from this equation is presented in figure 19. The ideal static-pressure rise across the rotor as a function of stagger angle and turning angle may be written as (reference 1)

$$\left(\frac{\Delta p_i}{q_f}\right)_r = \frac{1}{\cos^2 \beta} - \frac{1}{\cos^2 (\beta - \theta)} \qquad (7)$$

The ideal pressure rise across the stator is, if all rotation is assumed to be removed, equal to the kinetic energy of the tangential flow behind the rotor, or

$$\left(\frac{\Delta p_i}{q_f}\right)_s = \left(\frac{u}{V_f}\right)^2$$

$$= \left[\tan \beta_0 - \tan (\beta - \theta)\right]^2 \qquad (8)$$

The ideal pressure rise for the stage is

$$\left(\frac{\Delta p_i}{q_f}\right)_{r-s} = \left(\frac{\Delta p_i}{q_f}\right)_r + \left(\frac{\Delta p_i}{q_f}\right)_s \qquad (9)$$

When an initial rotation exists upstream of the stage, the stagger is altered and may be found from

$$\tan \beta = \tan \beta_0 - \tan \delta$$

For a given σc_l the new value of turning angle may then be determined in figure 19 and the pressure rise may be computed by substituting the altered values of stagger angle and turning angle in equations (7), (8), and (9).

APPENDIX C

DERIVATION OF THE FAN PERFORMANCE COEFFICIENTS, K_1 AND K_2

Consider the charts in figures 6 and 7. When the fan section diameter and rotational speed are specified as 3 feet and 1600 rpm, respectively, a given value of V_f/V_o and flight velocity V_o fixes the value of the rotational parameter N. Since $\Delta p_i/q_f$ is a function of N for a given σc_l relationship, the ordinate was computed by

$$\frac{\rho_o}{\rho_f}\frac{\Delta p_i}{q_o} = \frac{\Delta p_i}{q_f}\left(\frac{V_f}{V_o}\right)^2$$

When any other fan diameter and rotational speed are considered, the same relation between N and $\Delta p_i/q_f$ in the charts may be retained by redesignating the lines of constant V_f/V_o

$$K_1 = \frac{3}{d}\frac{1600}{n}\frac{V_f}{V_o}$$

The ordinate becomes $\frac{\Delta p_i}{q_f} K_1^2$, or in terms of free-stream dynamic pressure,

$$\frac{\Delta p_i}{q_f}\left(\frac{V_f}{V_o}\right)^2\left(\frac{1600}{n}\frac{3}{d}\right)^2 = \frac{\rho_o}{\rho_f}\frac{\Delta p_i}{q_o} - K_2$$

where

$$K_2 = \left(\frac{1600}{n}\frac{3}{d}\right)^2 = \left(\frac{K_1}{V_f/V_o}\right)^2$$

REFERENCES

1. Bogdonoff, Seymour M., and Bogdonoff, Harriet E.: Blade Design Data for Axial-Flow Fans and Compressors. NACA ACR No. L5F07a, 1945.

2. Mutterperl, William: High-Altitude Cooling. VI - Axial-Flow Fans and Cooling Power. NACA ARR No. L4I11e, 1944.

3. Bell, E. Barton, and DeKoster, Lucas J.: The Effect of Solidity, Blade Section, and Contravane Angle on the Characteristics of an Axial-Flow Fan. NACA ARR, Dec. 1942.

4. Zimney, Charles M., and Lappi, Viola M.: Data for Design of Entrance Vanes from Two-Dimensional Tests of Airfoils in Cascade. NACA ACR No. L5G18, 1945.

5. Glauert, H.: The Elements of Aerofoil and Airscrew Theory. Cambridge Univ. Press. 1926, pp. 14 - 15.

TABLE I

ILLUSTRATIVE EXAMPLE

	Item	Source	Stator-rotor	Rotor-stator	Rotor
	Propeller-speed fan; $\delta = 0°$				
(1)	K_{1_h}	Fig. 16	1.11	1.11	1.11
(2)	$\left(\frac{\rho_o}{\rho_f}\right) K_2 \frac{\Delta p_i}{q_o}$	Fig. 6	1.72	1.18	.58
(3)	$\frac{\rho_o}{\rho_f} \frac{\Delta p_i}{q_o}$	Fig. 17	.50	.35	.17
(4)	$\frac{\rho_f}{\rho_o}$	Equation 5	1.033	1.033	1.033
(5)	$\frac{\Delta p_i}{q_o}$	Items (3)×(4)	.52	.36	.18
	Propeller-speed fan; $\delta = 20°$				
(6)	$\left(\frac{\rho_o}{\rho_f}\right)\left(\frac{\Delta p_i' - \Delta p_i}{q_o}\right)$	Fig. 11	0.04	------	-----
(7)	β_{0_h}, deg.	Fig. 18	-------	35.	35.
(8)	$\frac{\Delta p_i - \Delta p_i'}{\Delta p_i}$	Fig. 14	-------	-.056	.97
(9)	$\frac{\Delta p_i}{q_o}$	Items [(4)×(6)]+(5)	.56	------	-----
		Items (5)-[(8)×(5)]	-------	.38	.01

TABLE I

ILLUSTRATIVE EXAMPLE - Concluded

	Item	Source	Stator-rotor	Rotor-stator	Rotor
	Geared fan; $\delta = 0^\circ$				
(10)	$\frac{\Delta p_i}{q_o}$ (required)	Specified	2.24	2.24	2.24
(11)	$\frac{\Delta p_i}{q_f}$	$\frac{\rho_o}{\rho_f} \frac{\Delta p_i}{q_o} \left(\frac{V_o}{V_f}\right)^2$	6.01	6.01	6.01
(12)	N_h	Fig. 5	1.98	2.51	2.94
(13)	Rotational speed, rpm	Item (12) $\times \frac{60 V_o \left(\frac{V_f}{V_o}\right)}{\pi d_h}$	3180	4040	4730
	Geared fan; $\delta = -20^\circ$				
(14)	$\frac{\rho_o}{\rho_f} \frac{\Delta p_i' - \Delta p_i}{q_o}$	Fig. 11	0.04	------	-----
(15)	K_{l_h}	Fig. 16	-------	0.31	0.26
(16)	β_{0_h}, deg	Fig. 18	-------	68	71
(17)	$\frac{\Delta p_i' - \Delta p_i}{\Delta p_i}$	Fig. 15	-------	.11	.25
(18)	$\frac{\Delta p_i}{q_o}$	Items [(4)×(14)]+(10)	2.28	------	-----
		Items [(10)×(17)]+(10)	-------	2.49	2.80

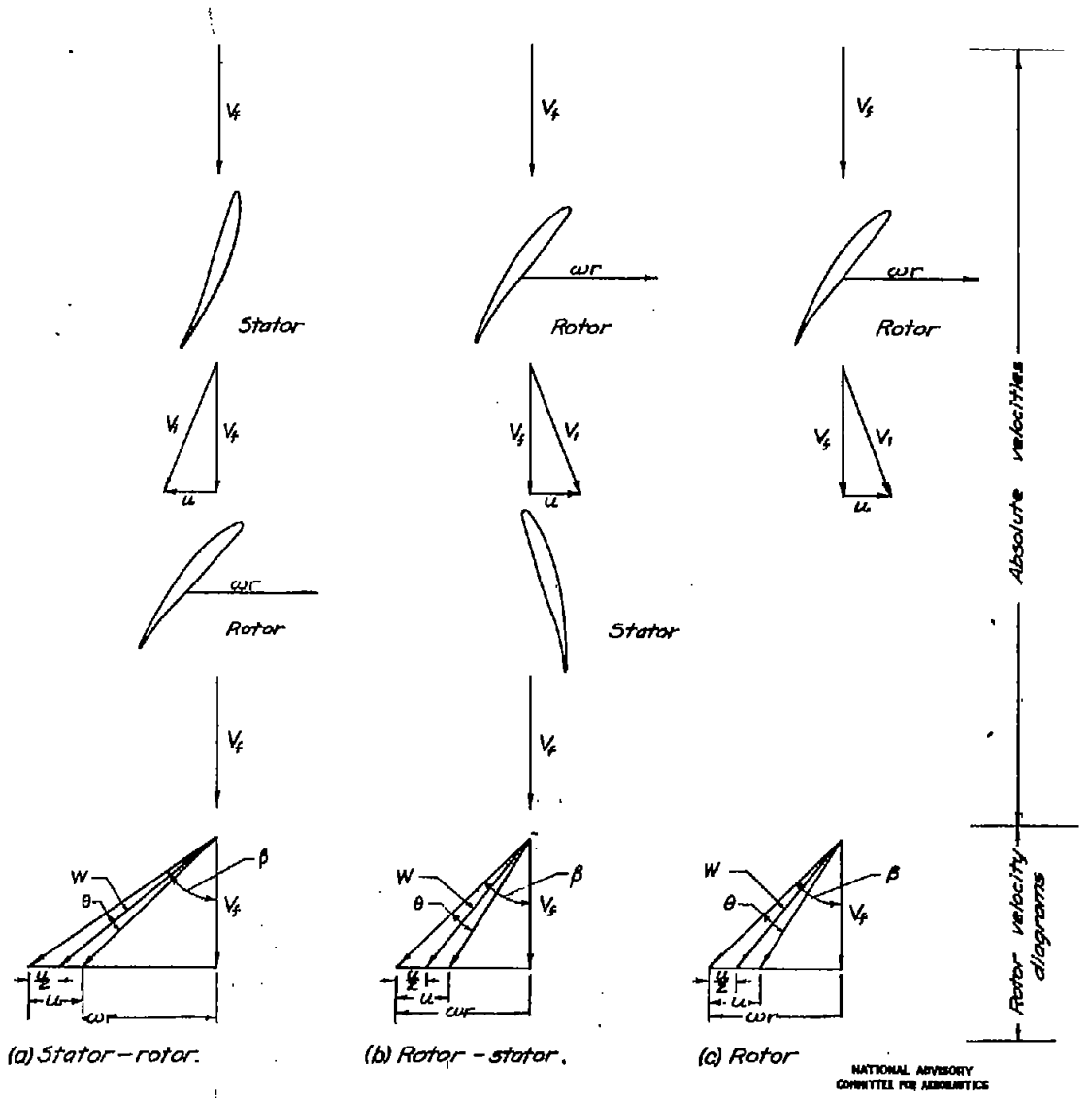

Figure 1.- Velocity diagrams for stator-rotor, rotor-stator, and rotor fans.

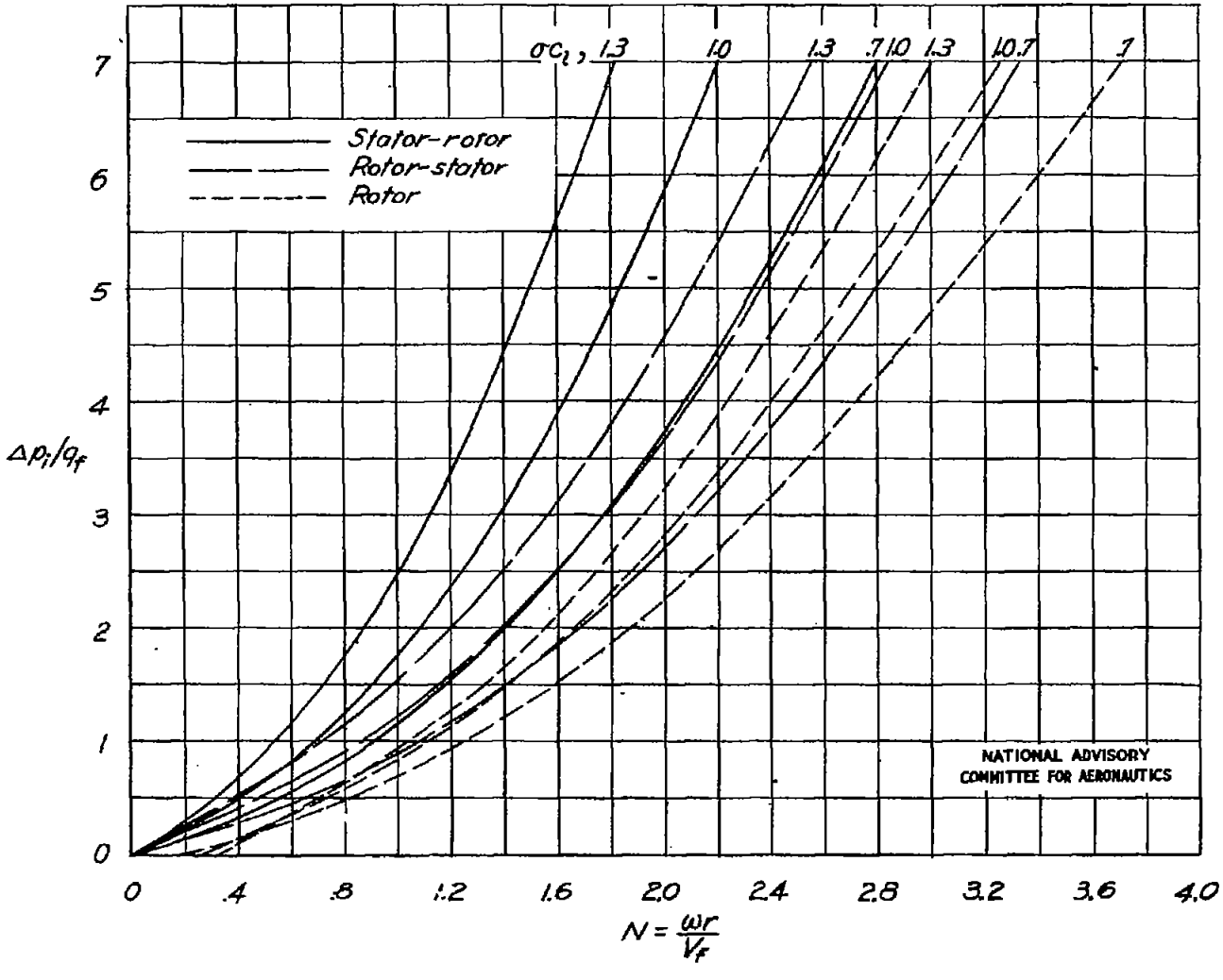

(a) Low N.

Figure 2.- Variation of ideal pressure-rise coefficient with N for stator-rotor, rotor-stator, and rotor at σc_l of 0.7, 1.0, and 1.3. (From reference 2.)

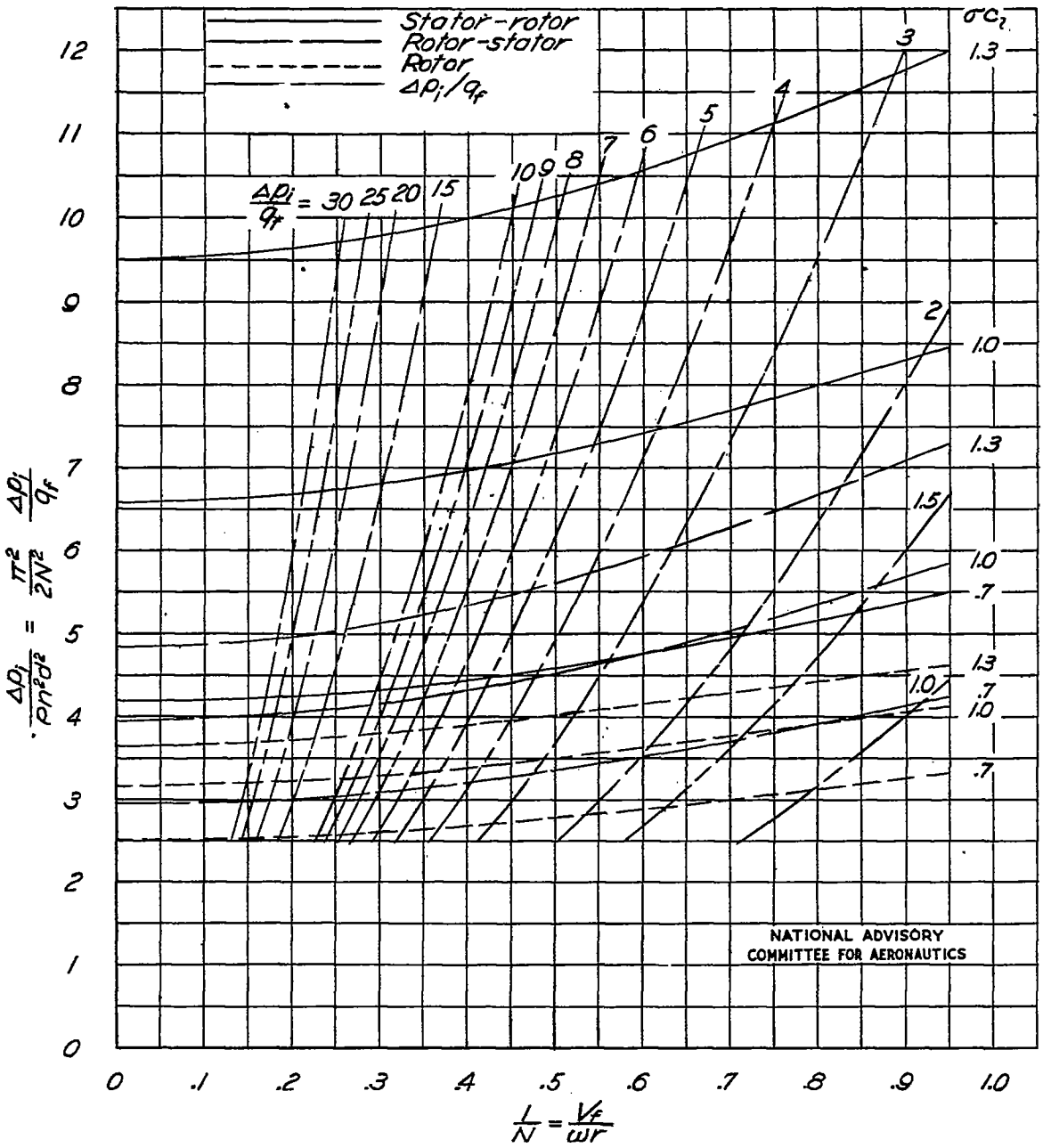

(b) High N. (Values of n are expressed in rps.)

Figure 2.- Concluded.

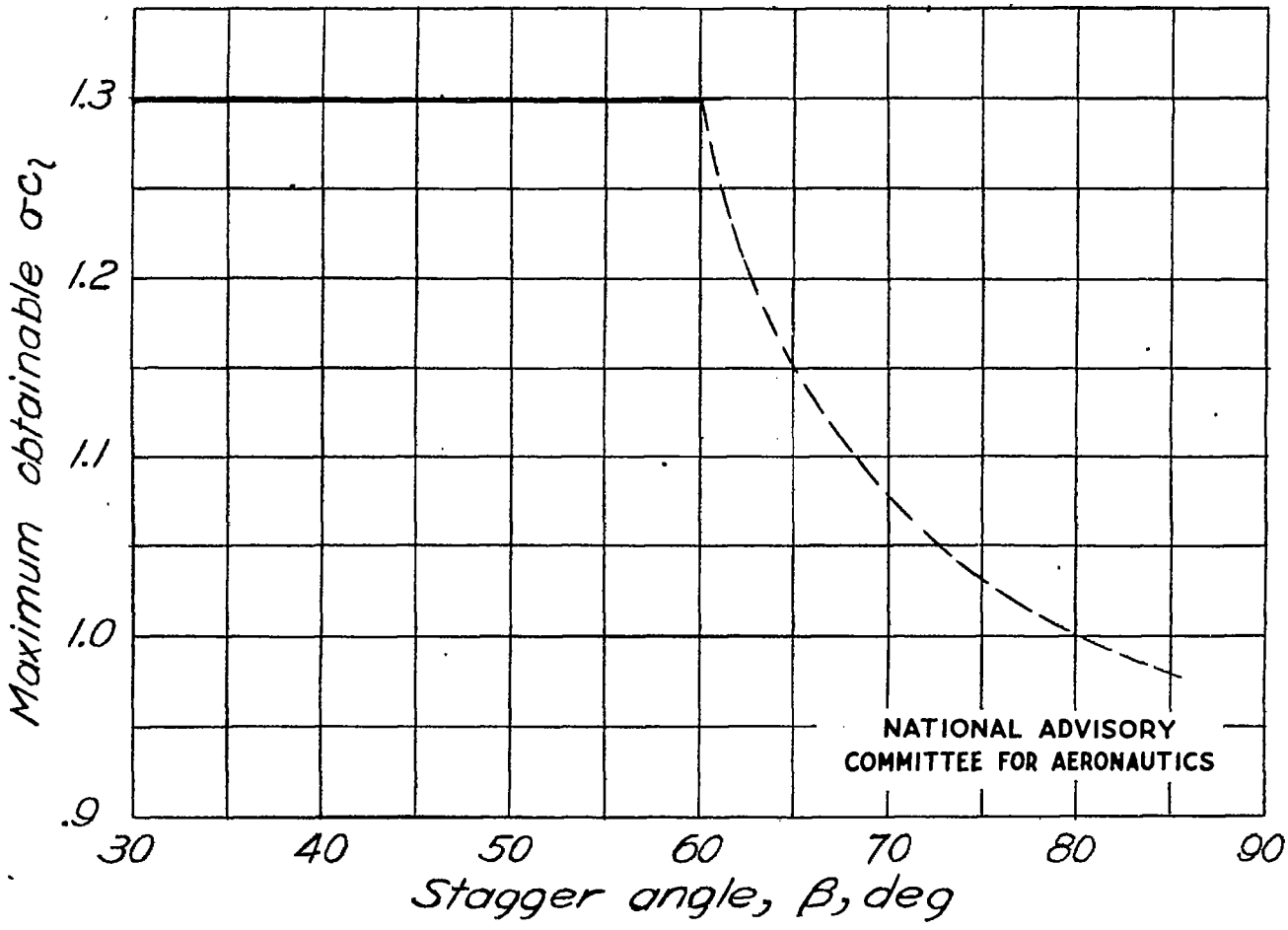

Figure 3.- Variation of maximum obtainable σc_l with stagger angle.

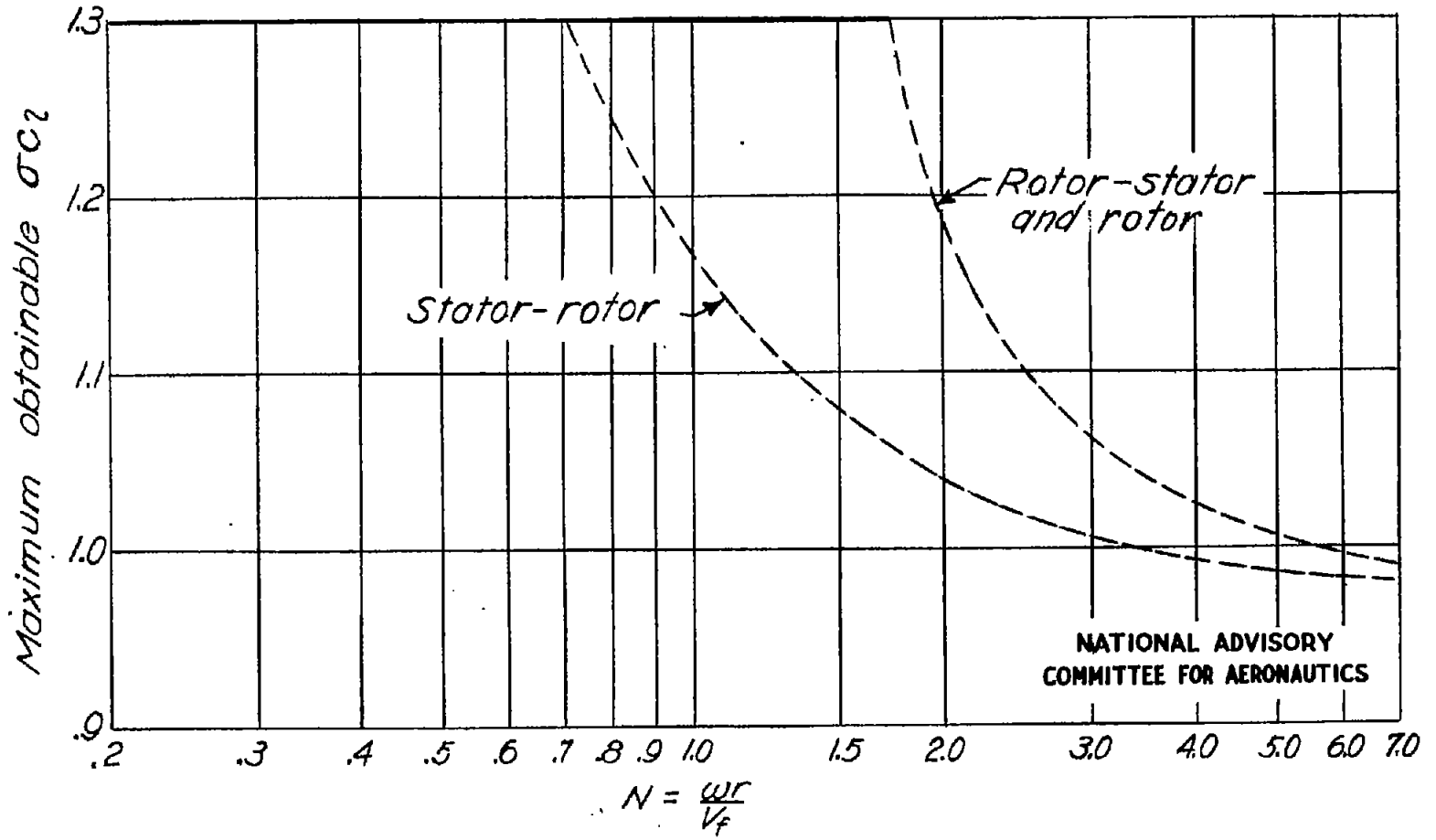

Figure 4.- Variation of maximum obtainable σc_l with N for stator-rotor, rotor-stator, and rotor.

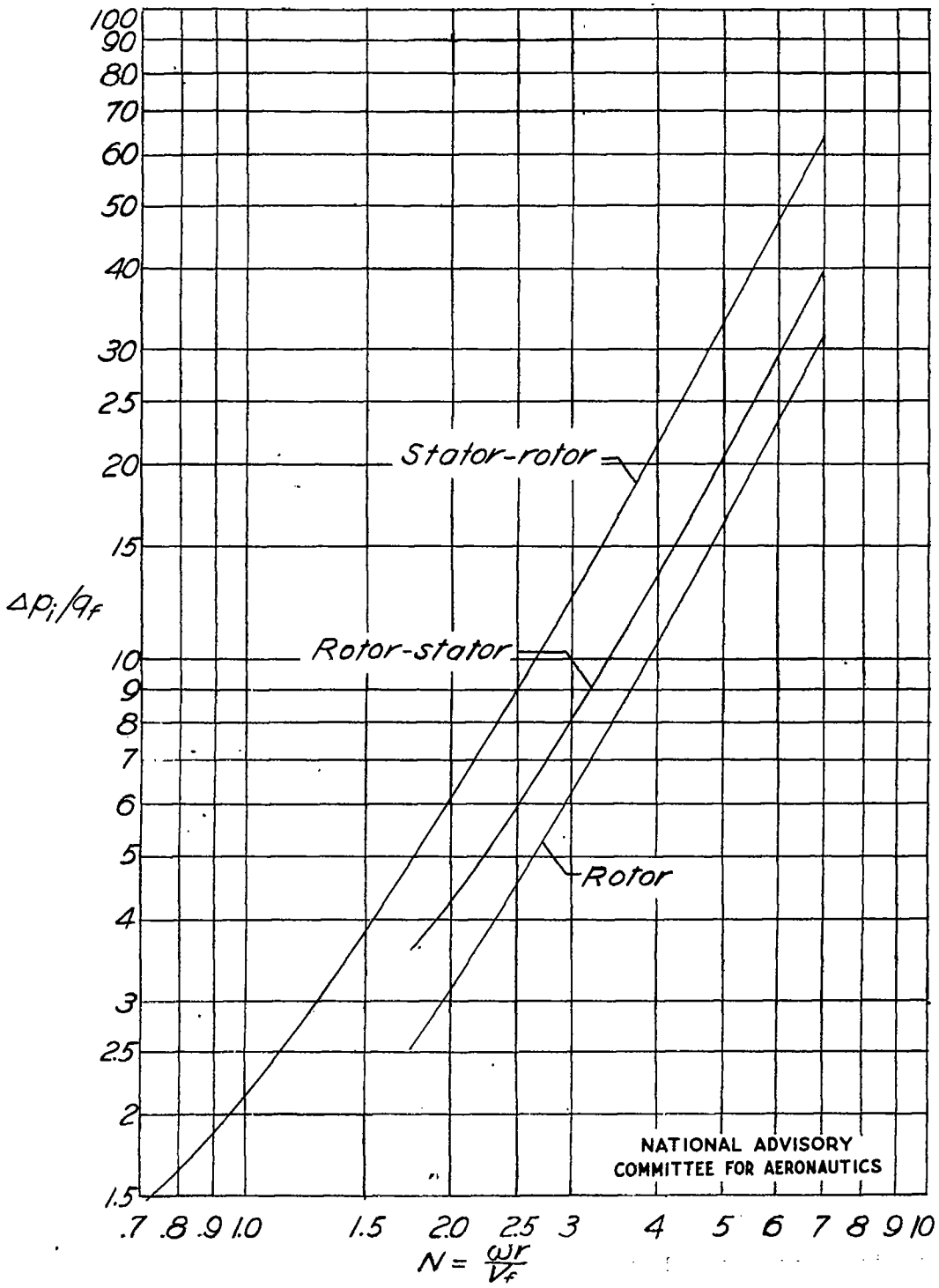

Figure 5.- Variation of maximum obtainable ideal pressure-rise coefficient with N for stator-rotor, rotor-stator, and rotor for stagger angles greater than 60°.

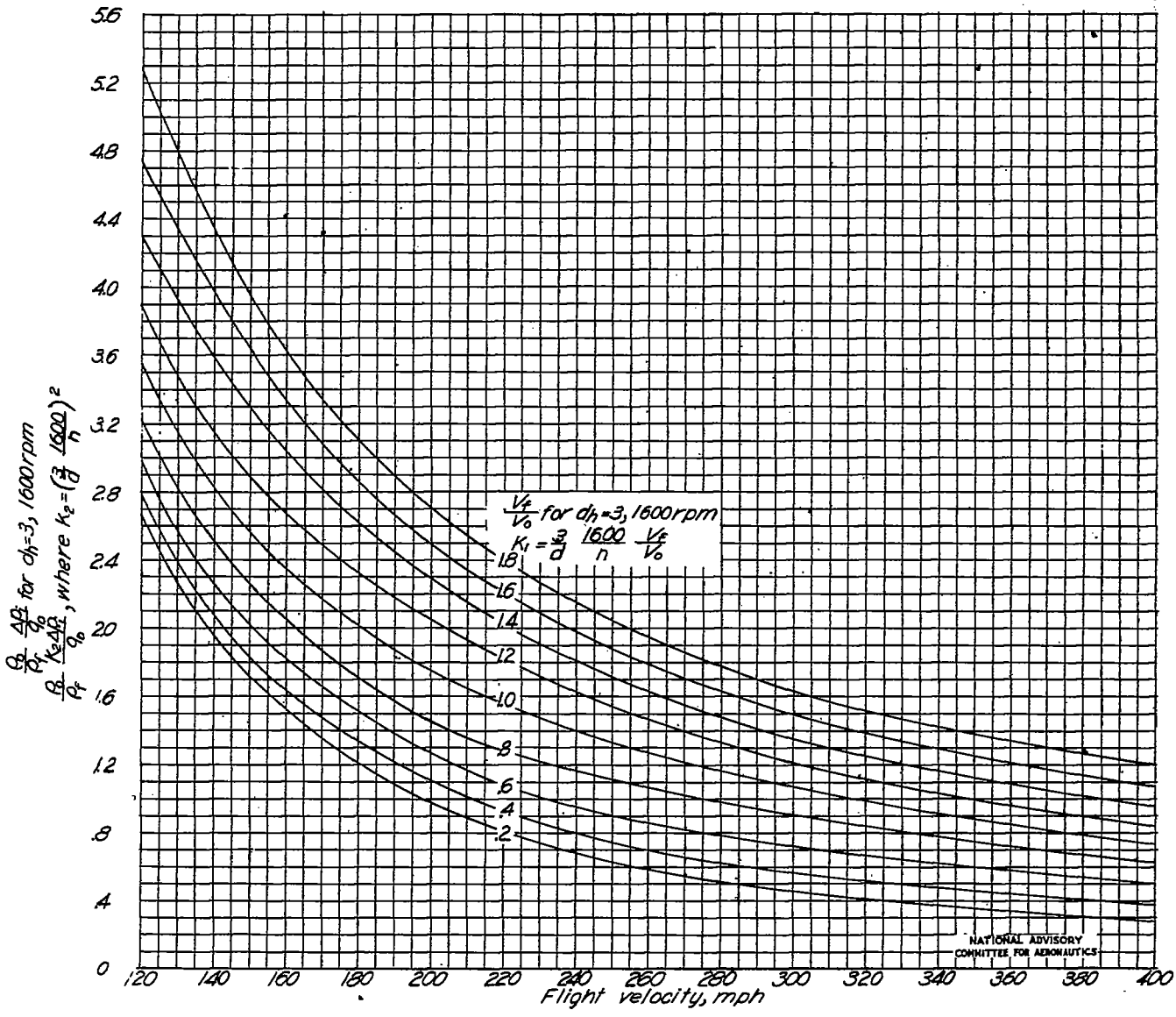

(a) Stator-rotor.

Figure 6.- Variation of maximum obtainable ideal pressure-rise coefficient with V_f/V_o and flight velocity for typical propeller-speed fan.

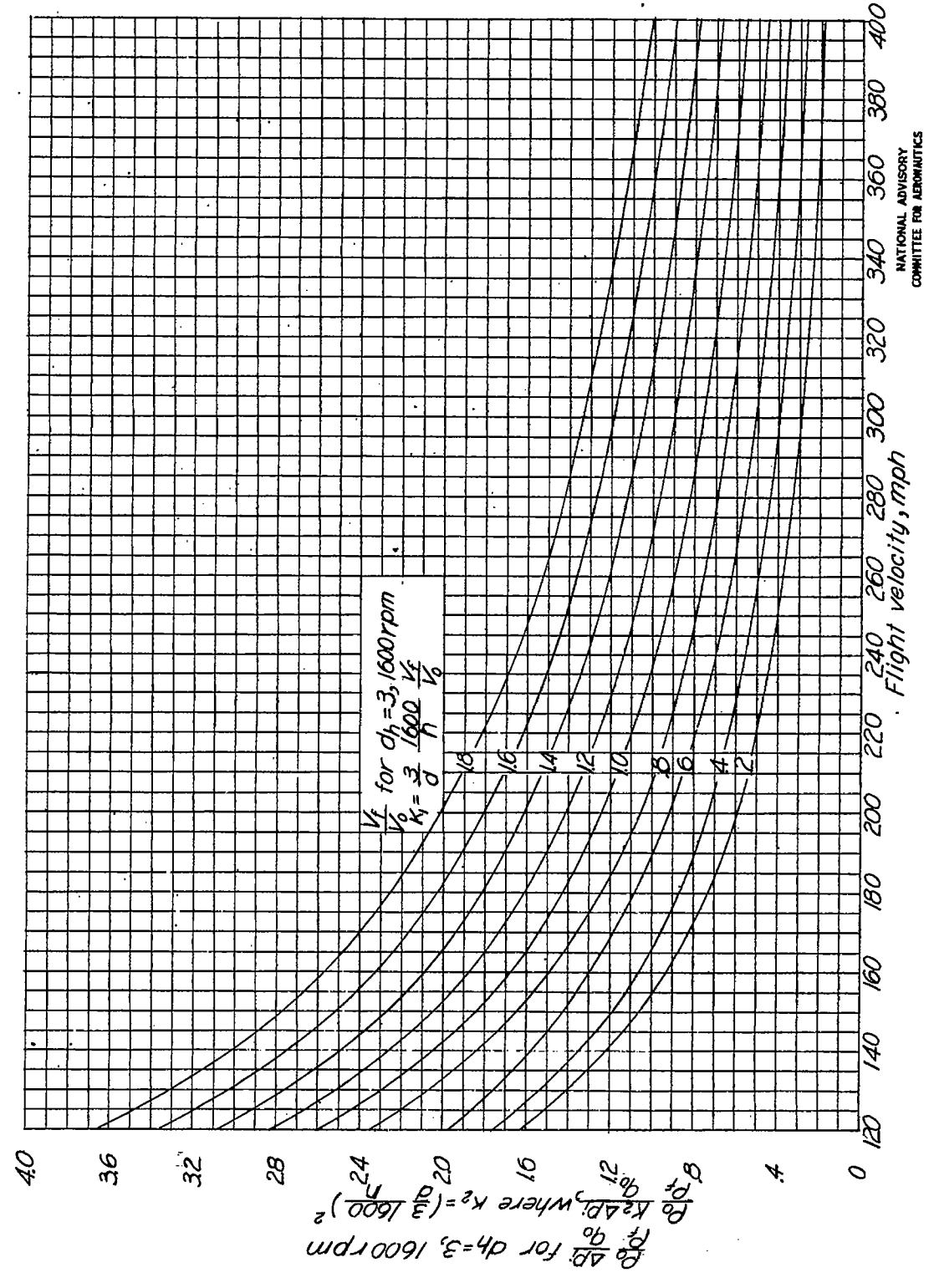

(b) Rotor-stator.

Figure 6.- Continued.

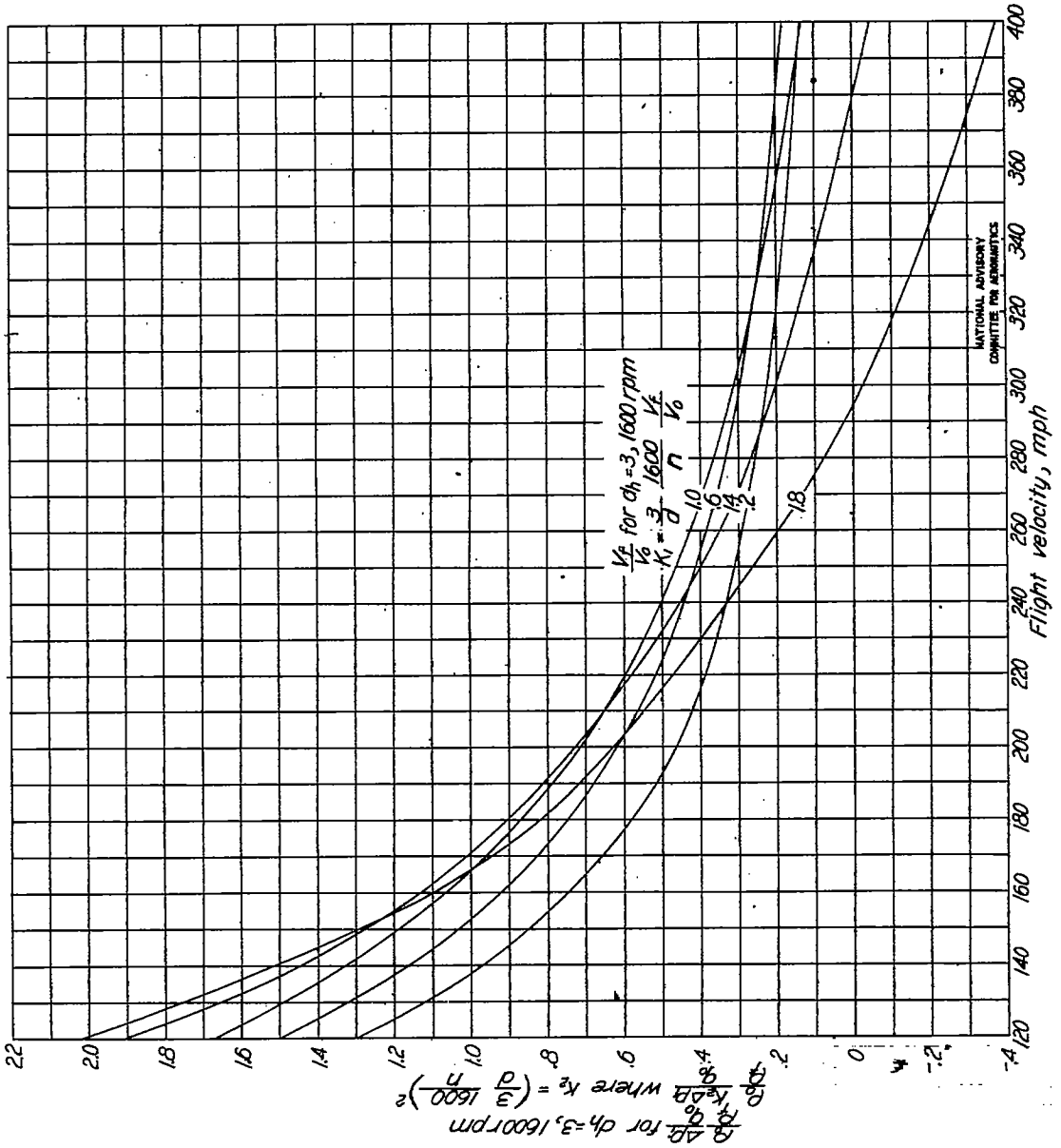

(c) Rotor.

Figure 6.- Concluded.

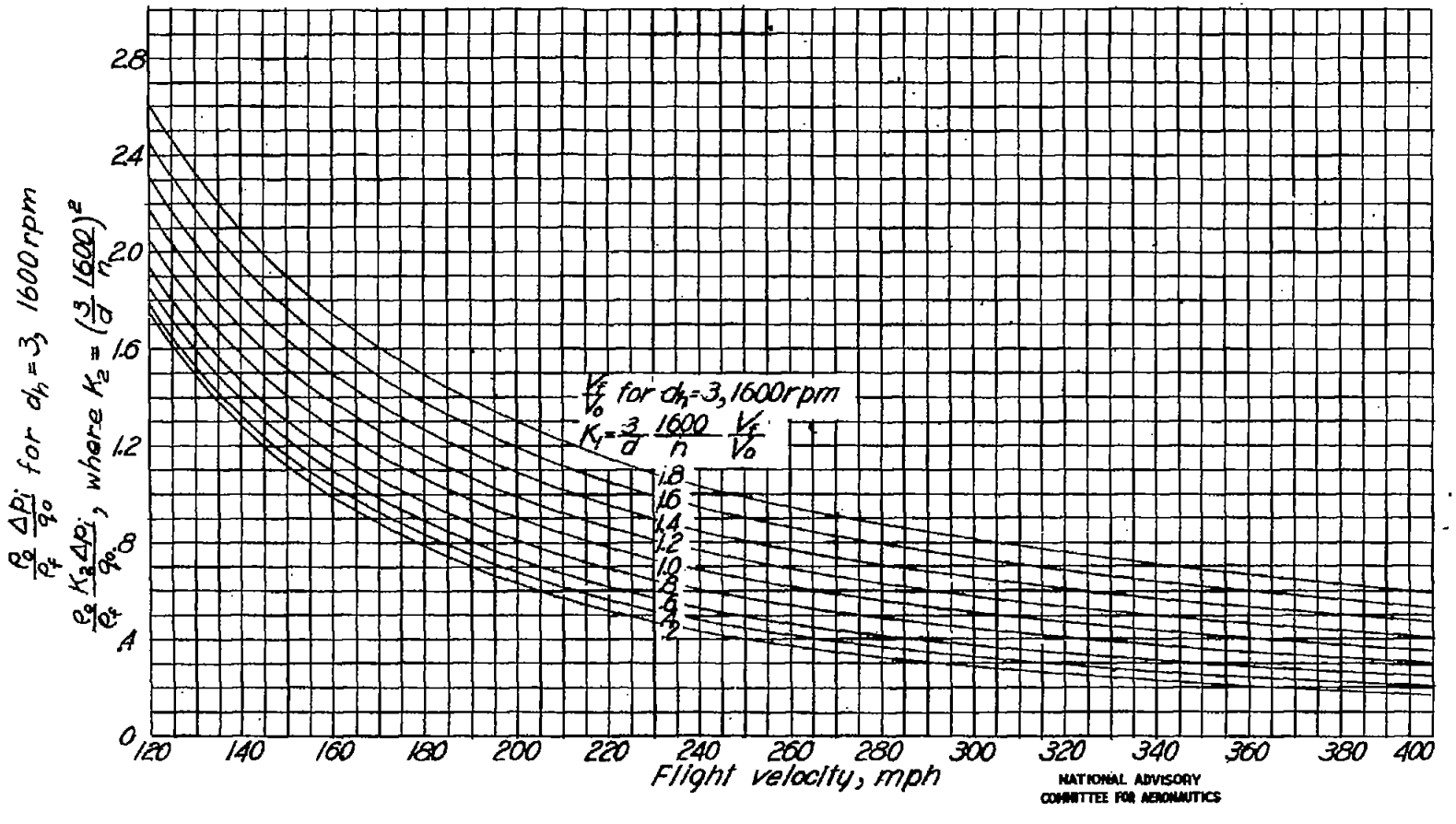

(a) Stator-rotor.

Figure 7.- Variation of maximum obtainable ideal pressure-rise coefficient with V_f/V_o and flight velocity for typical propeller-speed fan with low cambered sections. $\sigma c_l = 0.7$; $d_h = 3$ feet; rotational speed, 1600 rpm.

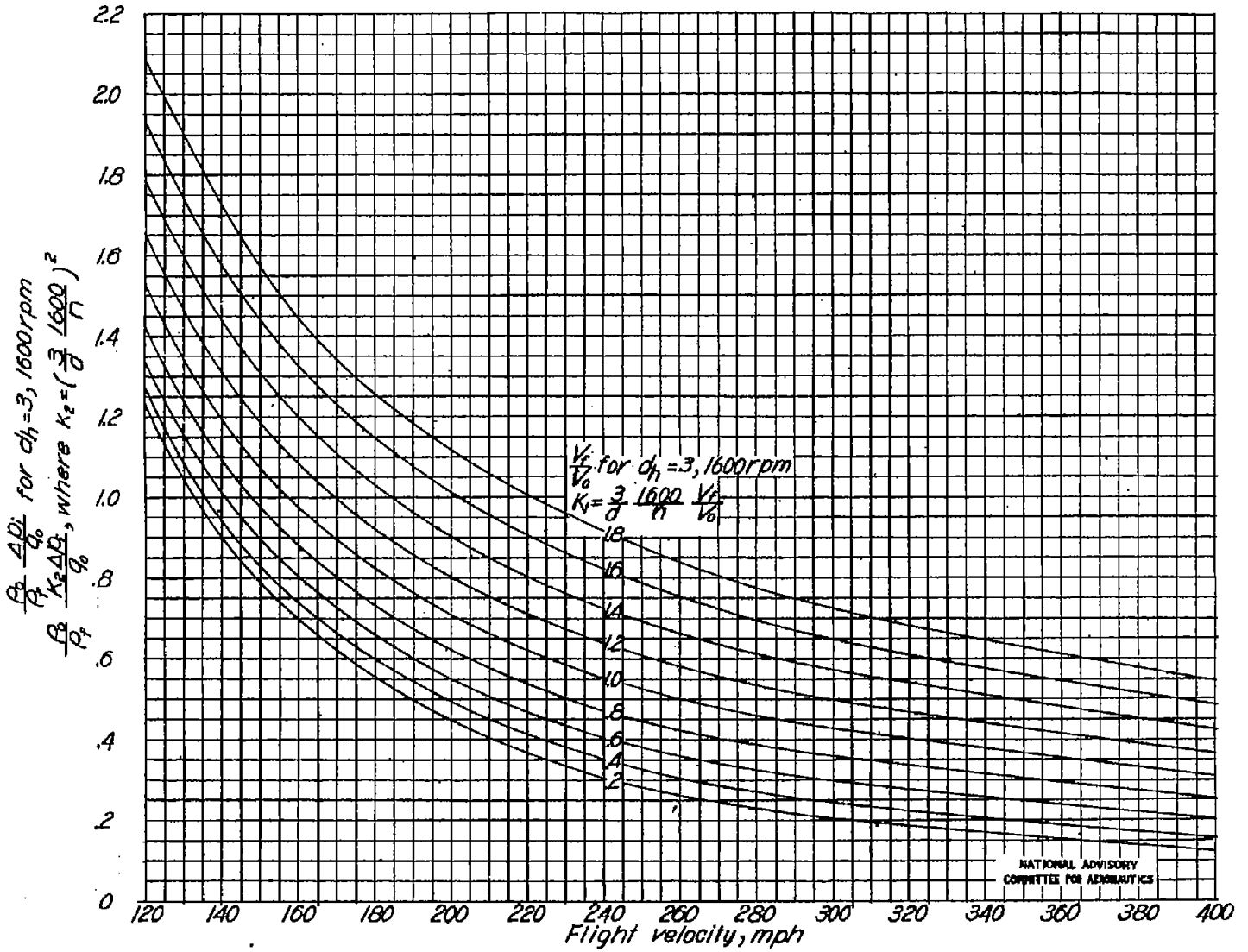

(b) Rotor-stator.

Figure 7.- Continued.

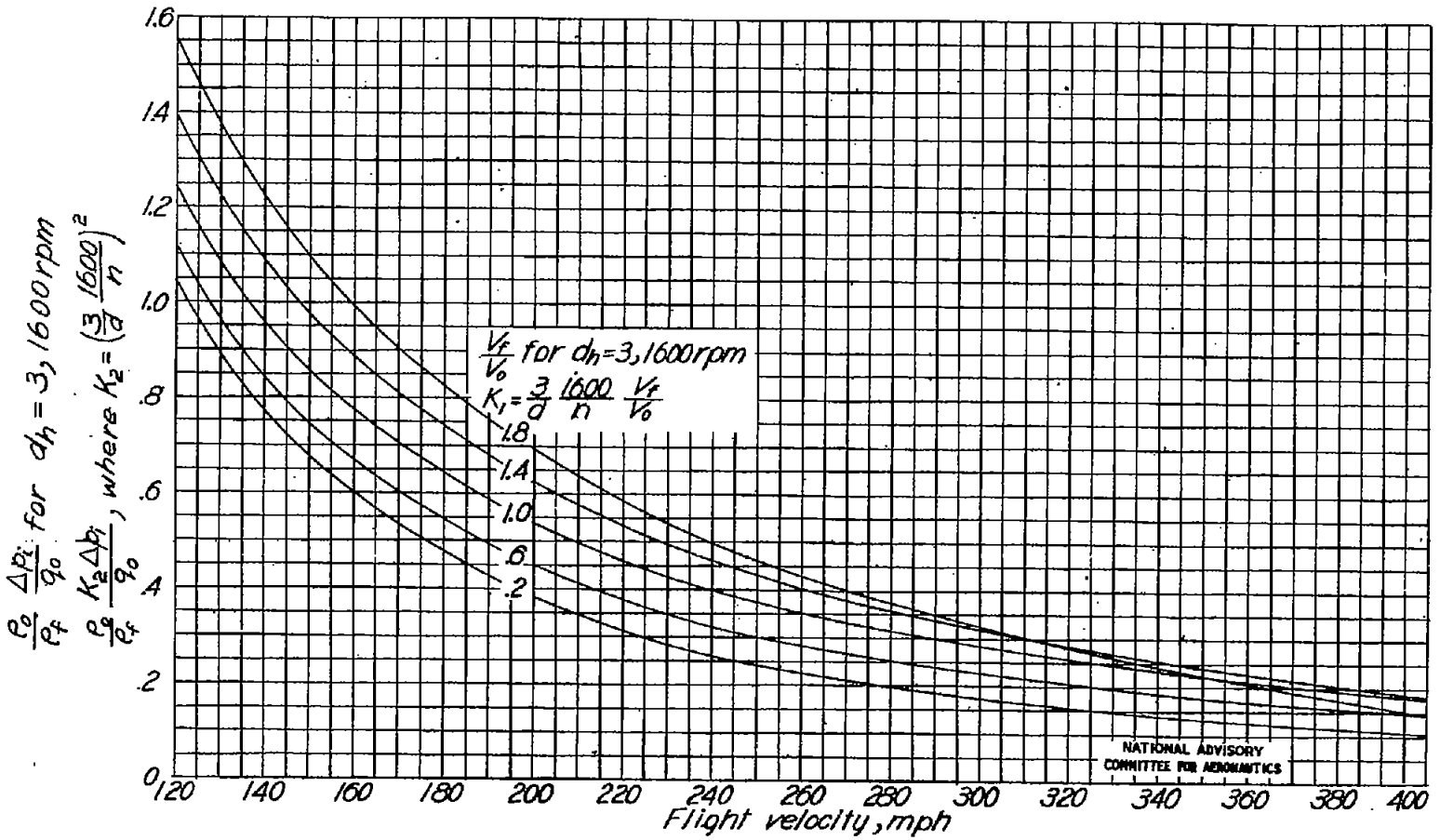

(c) Rotor.

Figure 7.- Concluded.

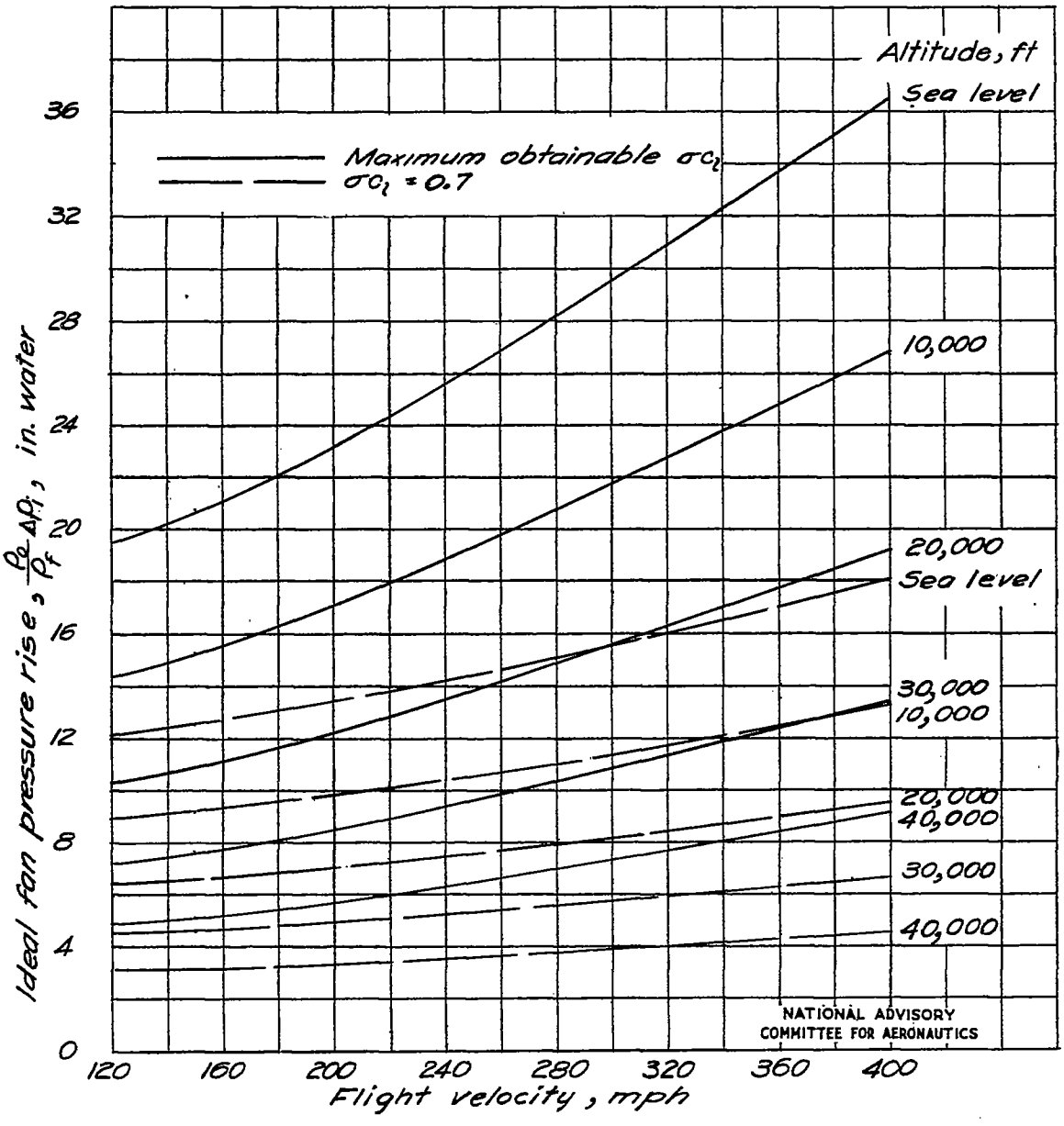

(a) Stator-rotor.

Figure 8.- Variation of fan pressure rise in inches of water, Army standard air, with flight velocity and altitude for typical propeller-speed fan, d_h = 3.0 feet, 1600 rpm, $\frac{V_f}{V_o}$ = 0.6.

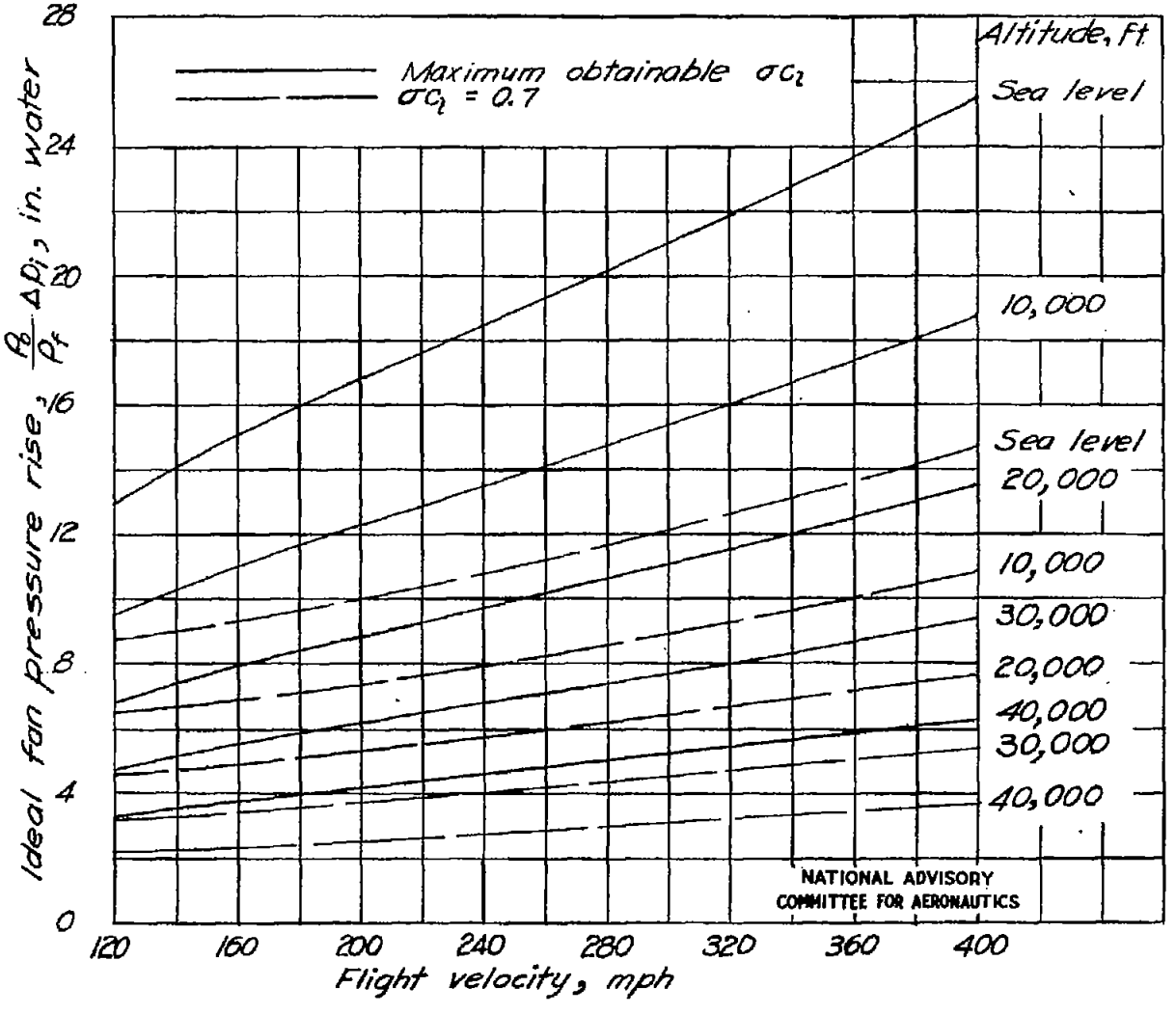

(b) Rotor-stator.

Figure 8.- Continued.

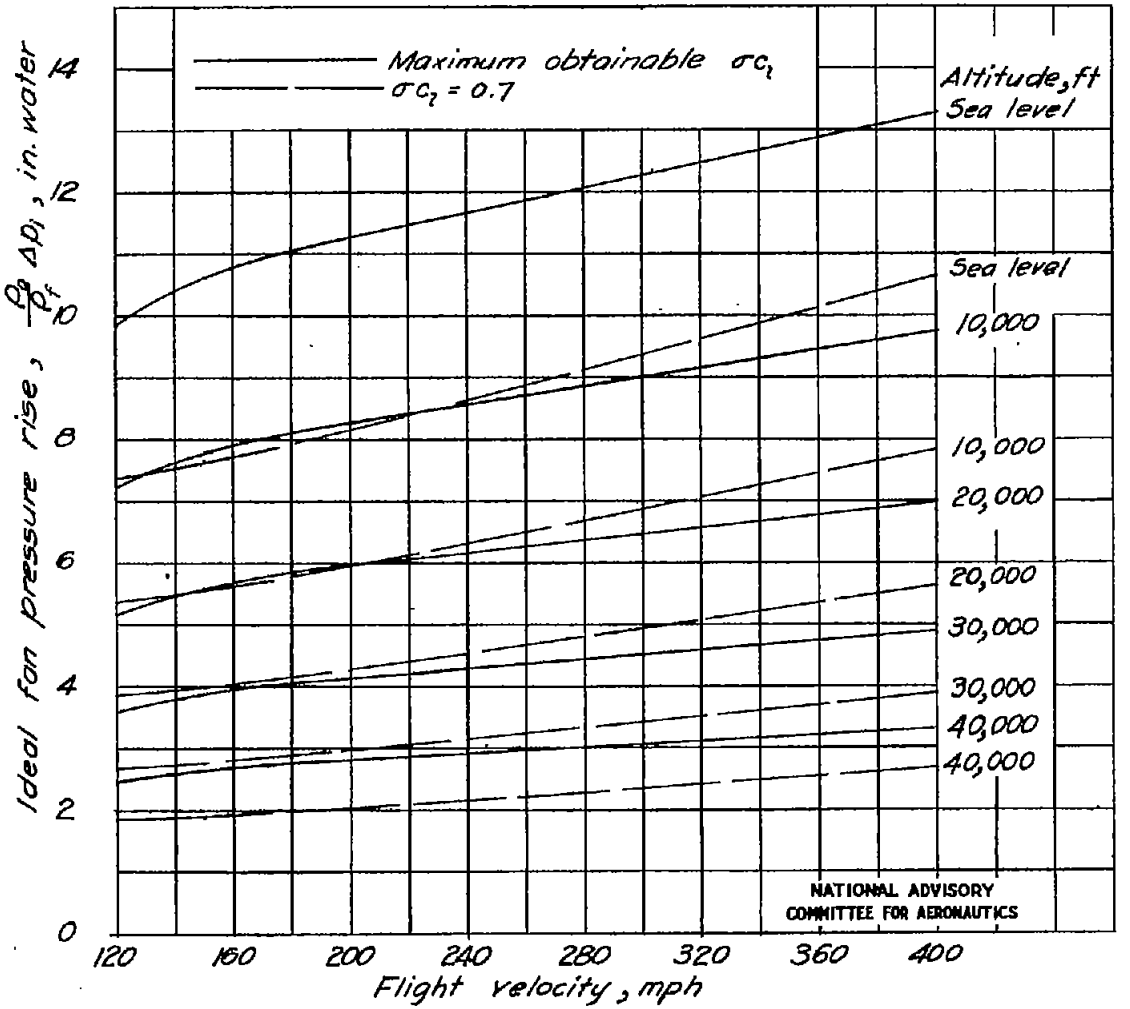

(c) Rotor.

Figure 8.- Concluded.

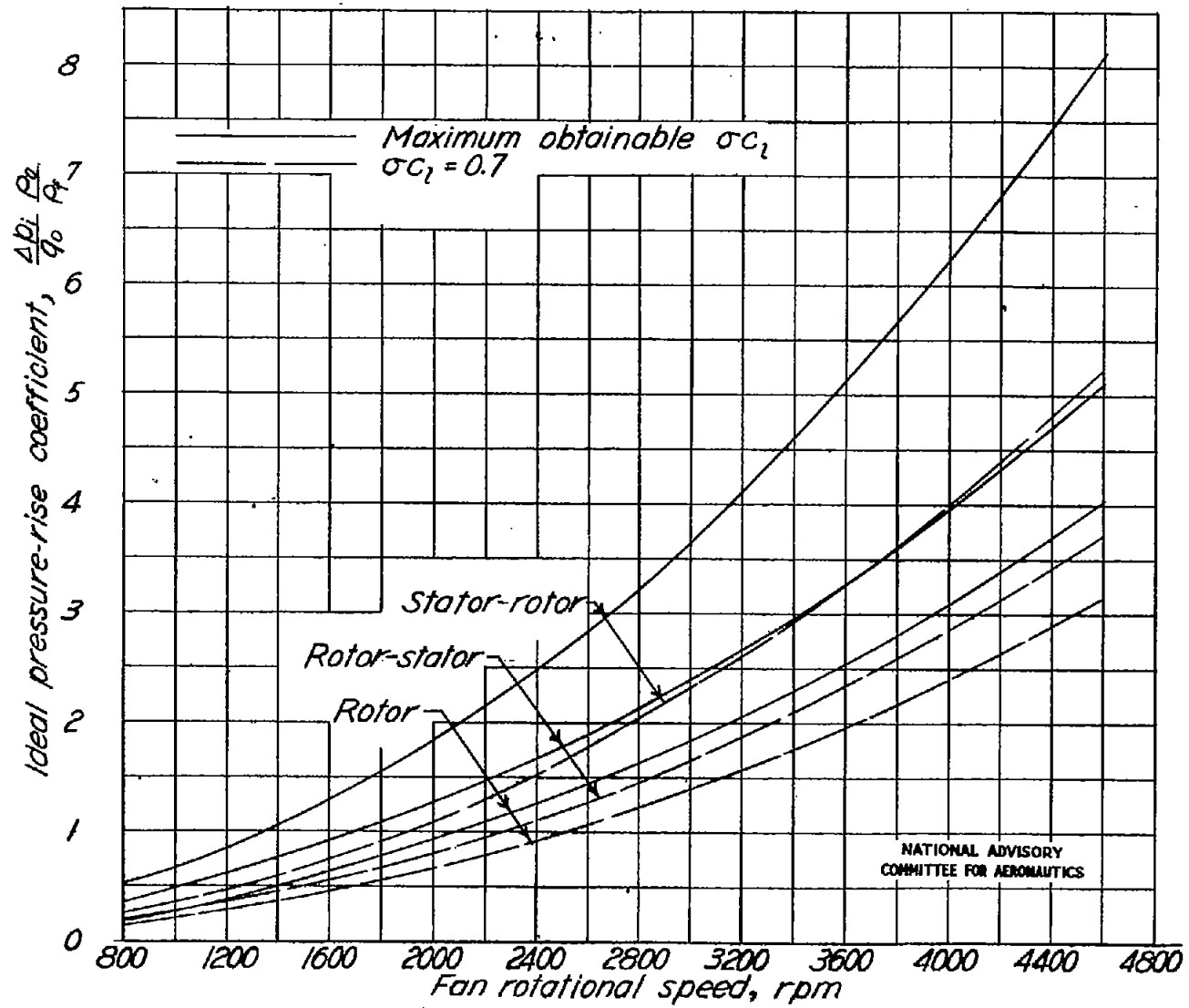

Figure 9.- Variation of ideal pressure-rise coefficient with rotational speed at 200 miles per hour flight velocity. $\frac{V_f}{V_o} = 0.6$; $d_h = 3.0$ feet.

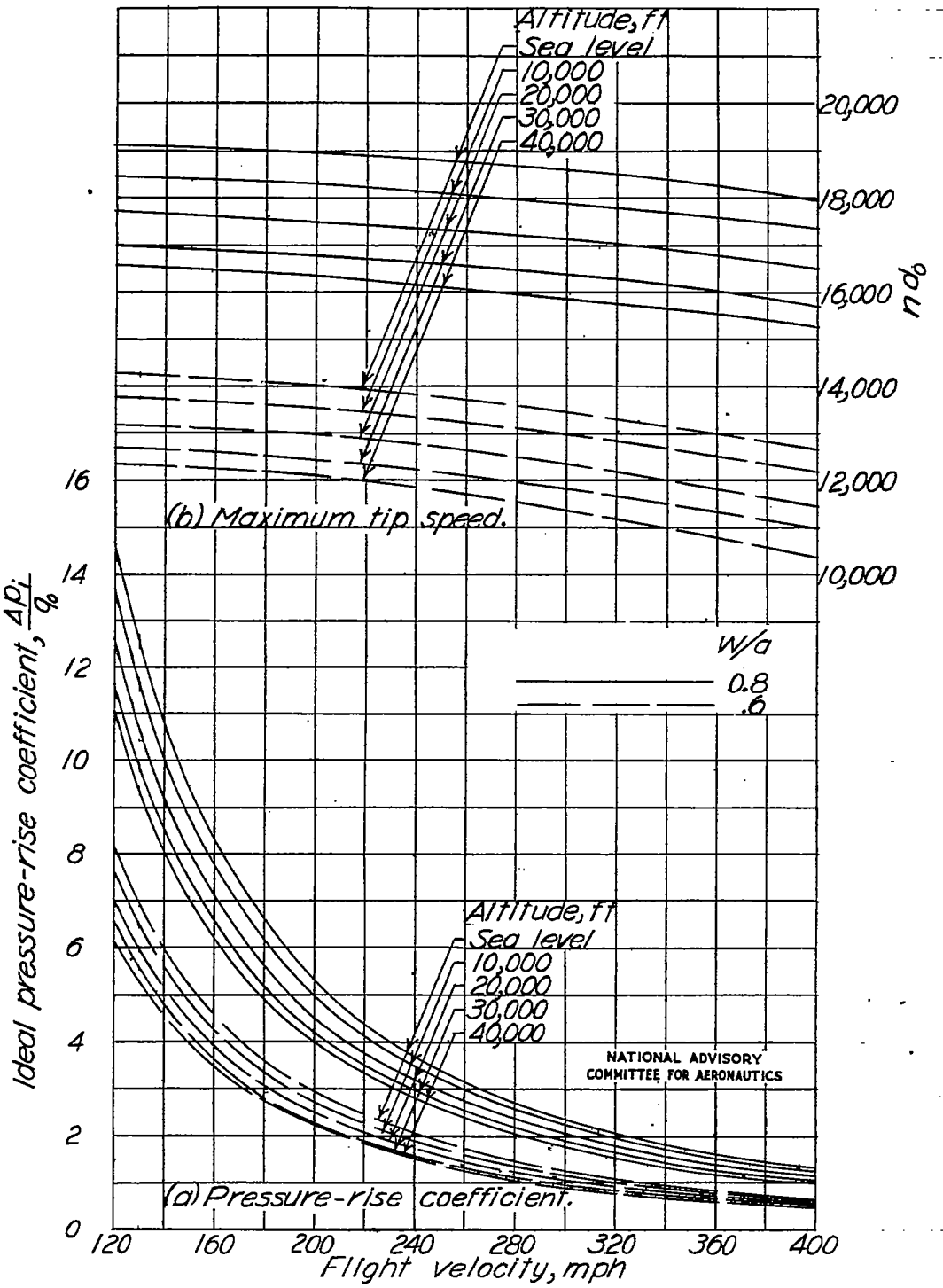

Figure 10.- Variation of maximum ideal pressure rise and maximum tip speed with flight velocity and altitude as limited by compressibility effects. $\frac{V_f}{V_o} = 0.6$.

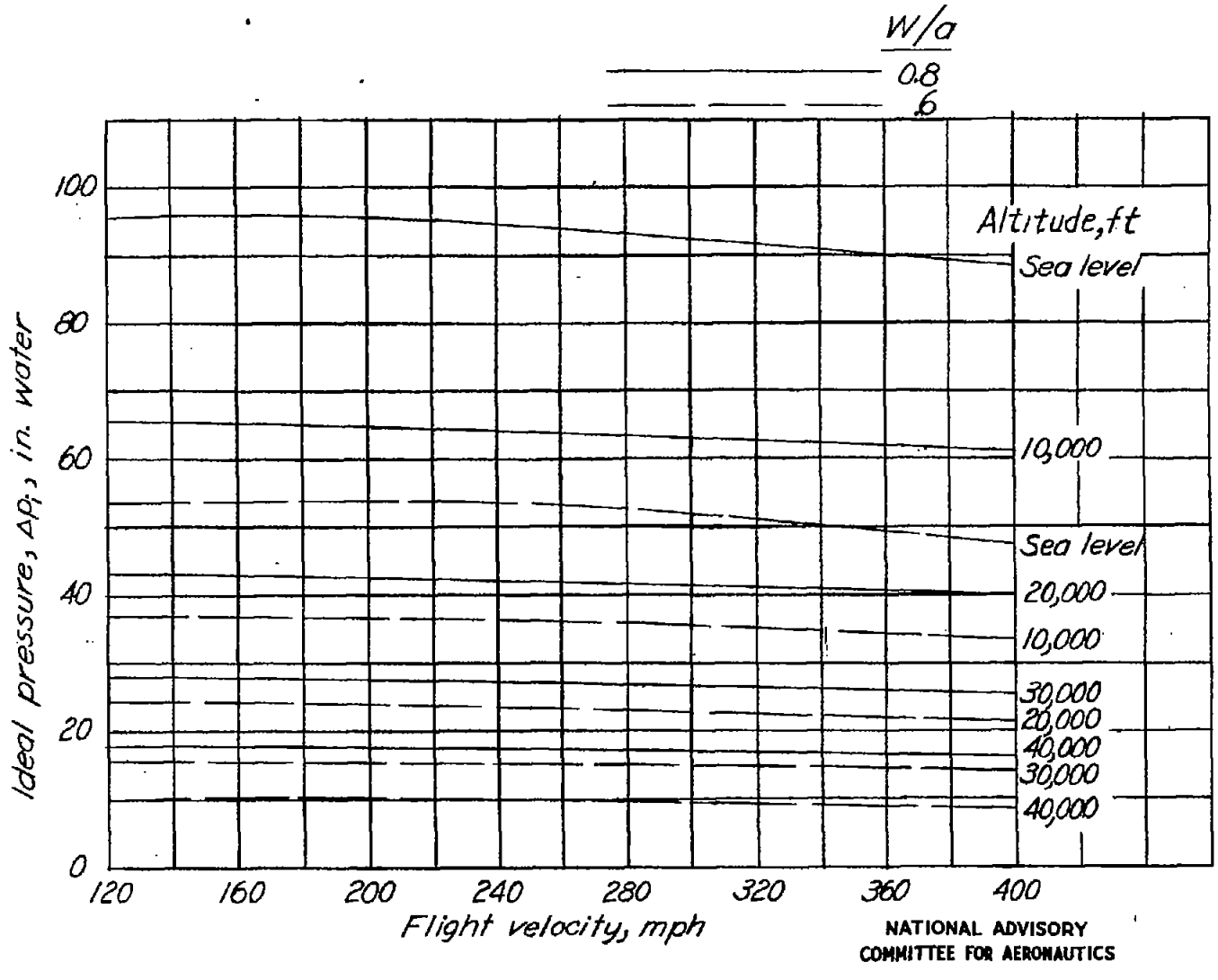

(c) Pressure rise, inches of water, Army standard air.

Figure 10.- Concluded.

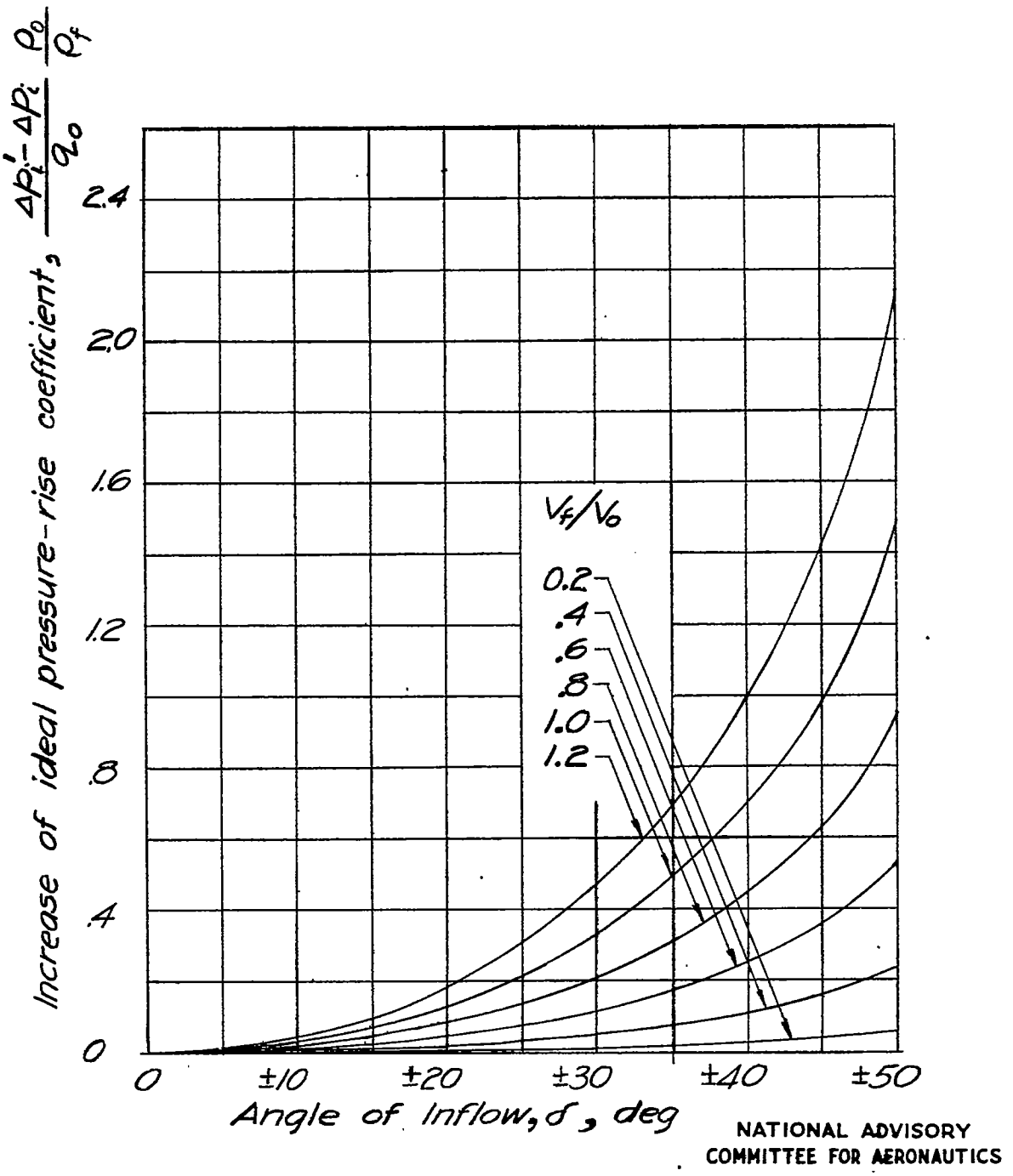

Figure 11.- Increase of stator-rotor ideal pressure-rise coefficient due to initial rotational inflow.

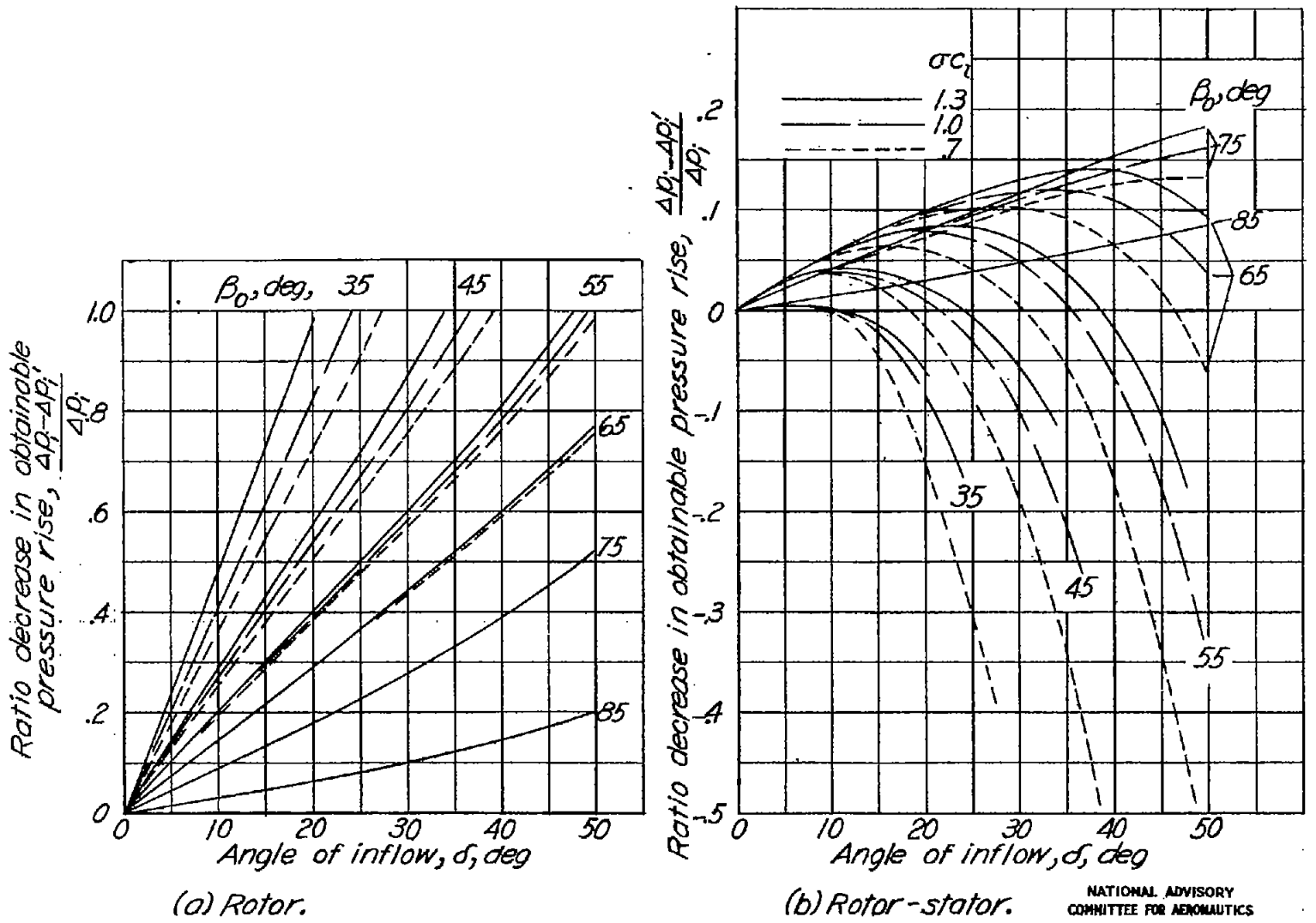

Figure 12.- Ratio decrease of ideal pressure rise for rotor and rotor-stator due to initial rotational inflow in the same direction as fan rotation.

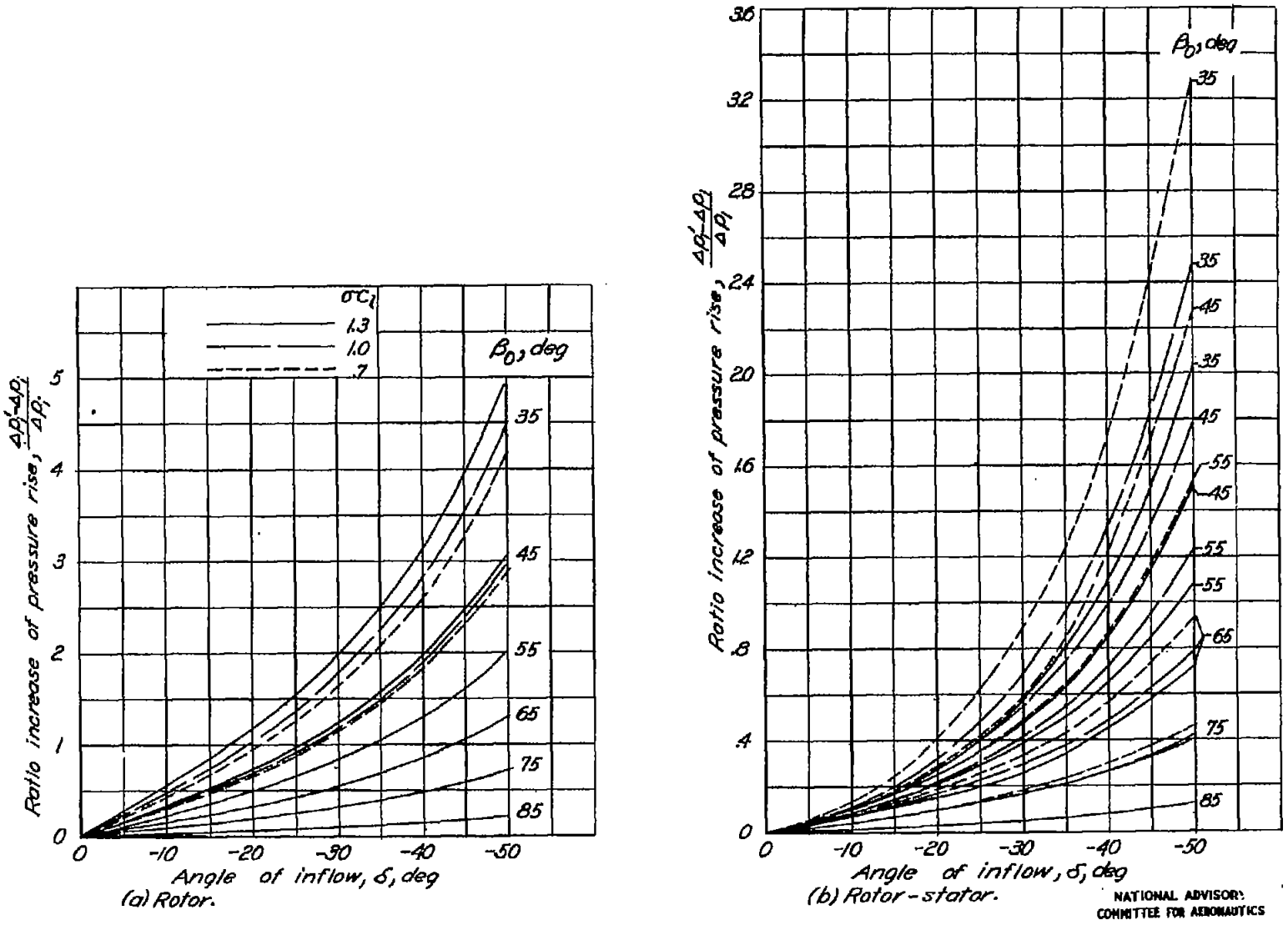

Figure 13.- Ratio increase of ideal pressure rise for rotor and rotor-stator due to initial rotational inflow in the direction opposite to fan rotation.

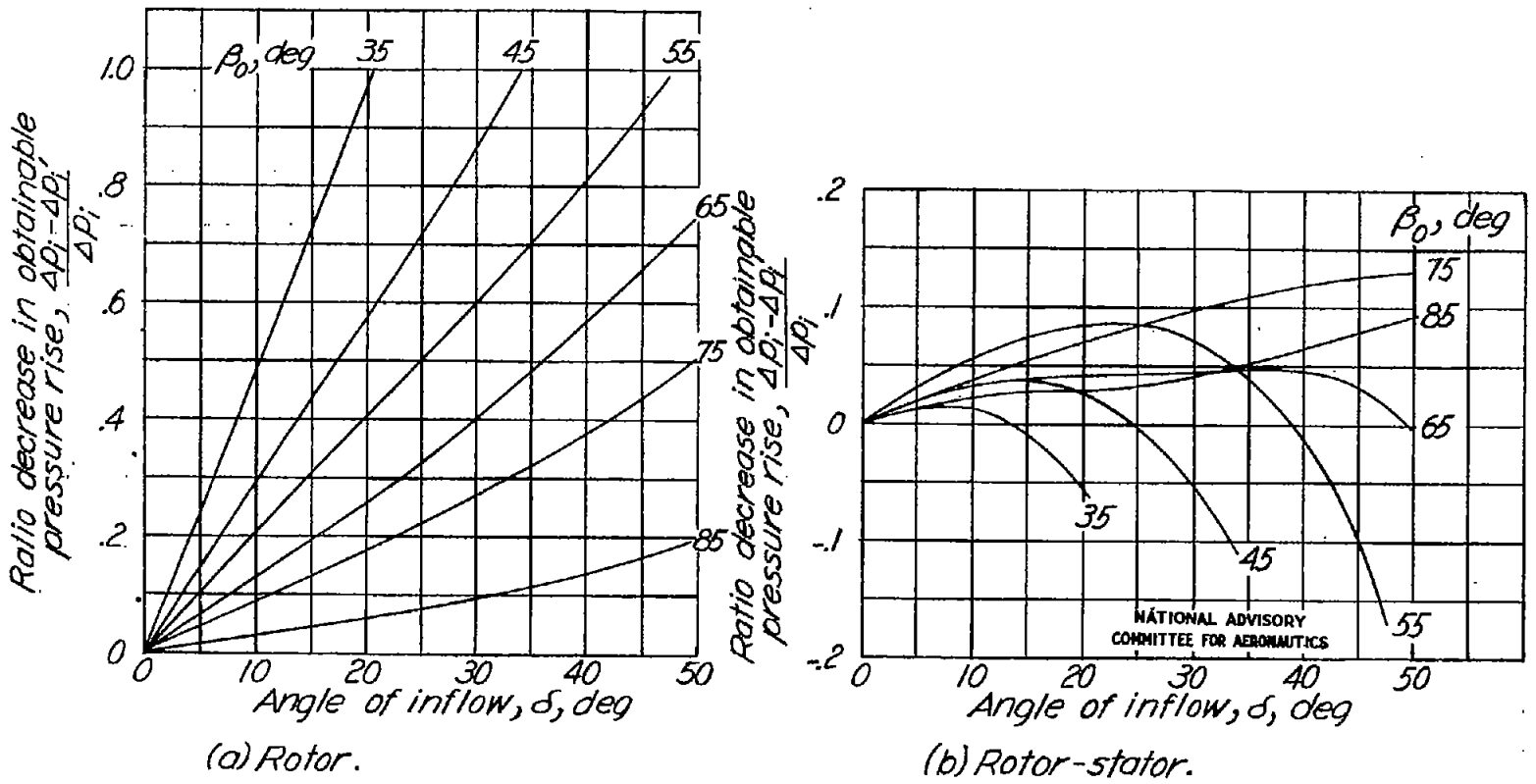

Figure 14.- Ratio decrease of ideal pressure rise for rotor and rotor-stator due to initial rotational inflow in the same direction as fan rotation for maximum obtainable σc_l.

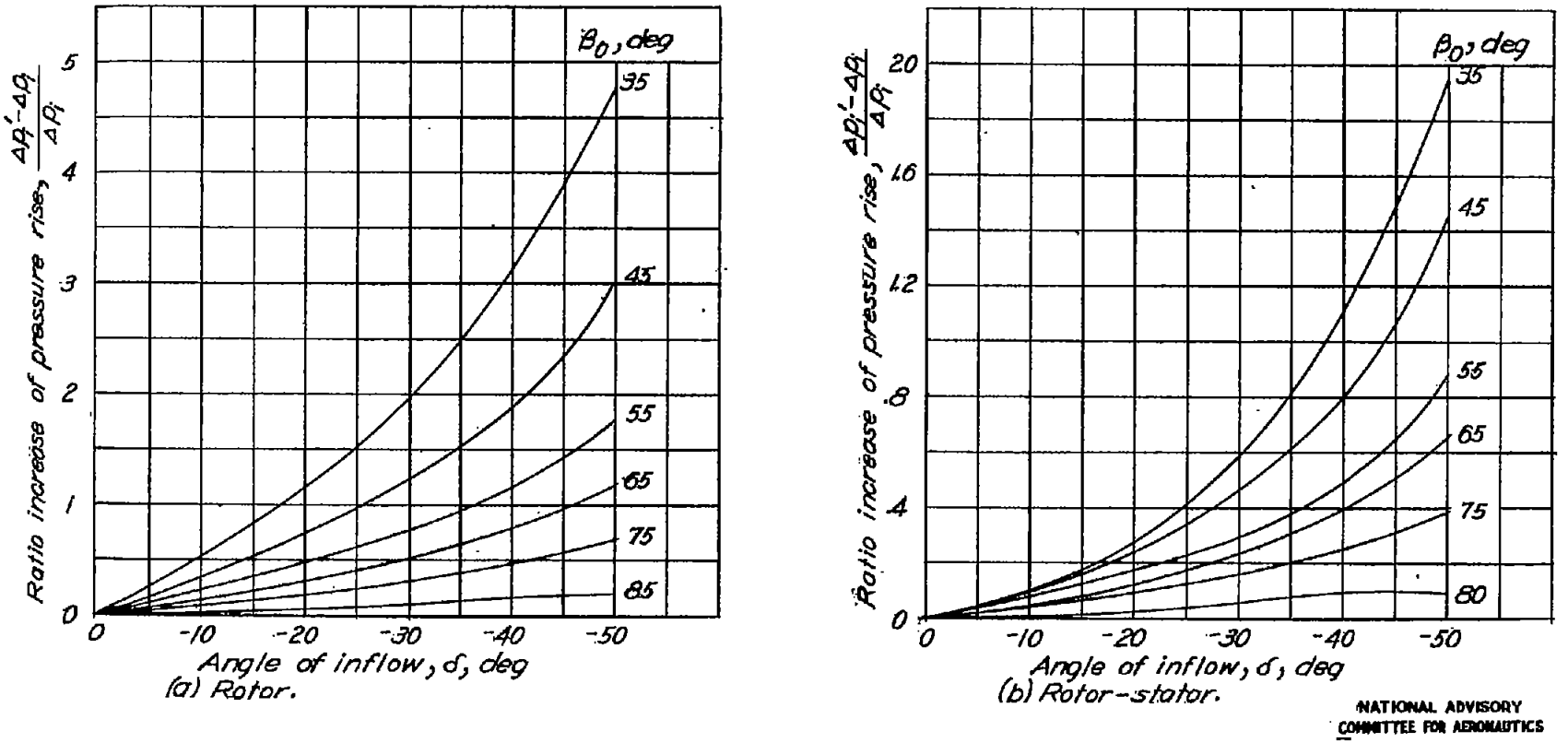

Figure 15.- Ratio increase of ideal pressure rise for rotor and rotor-stator due to initial rotational inflow in the direction opposite to fan rotation for maximum obtainable σc_l.

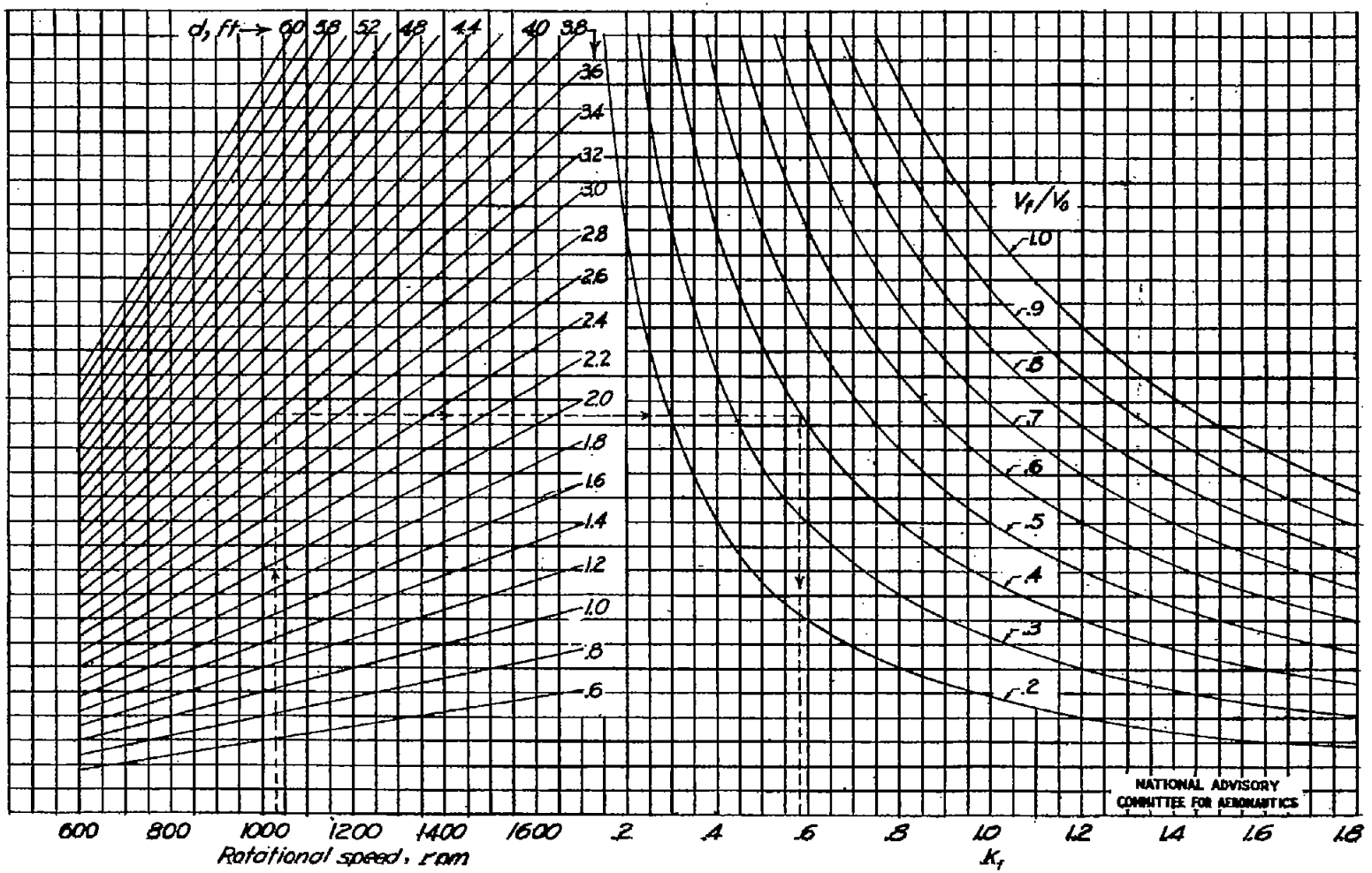

(a) Low rotational speed.

Figure 16.- Charts for determining K_1.

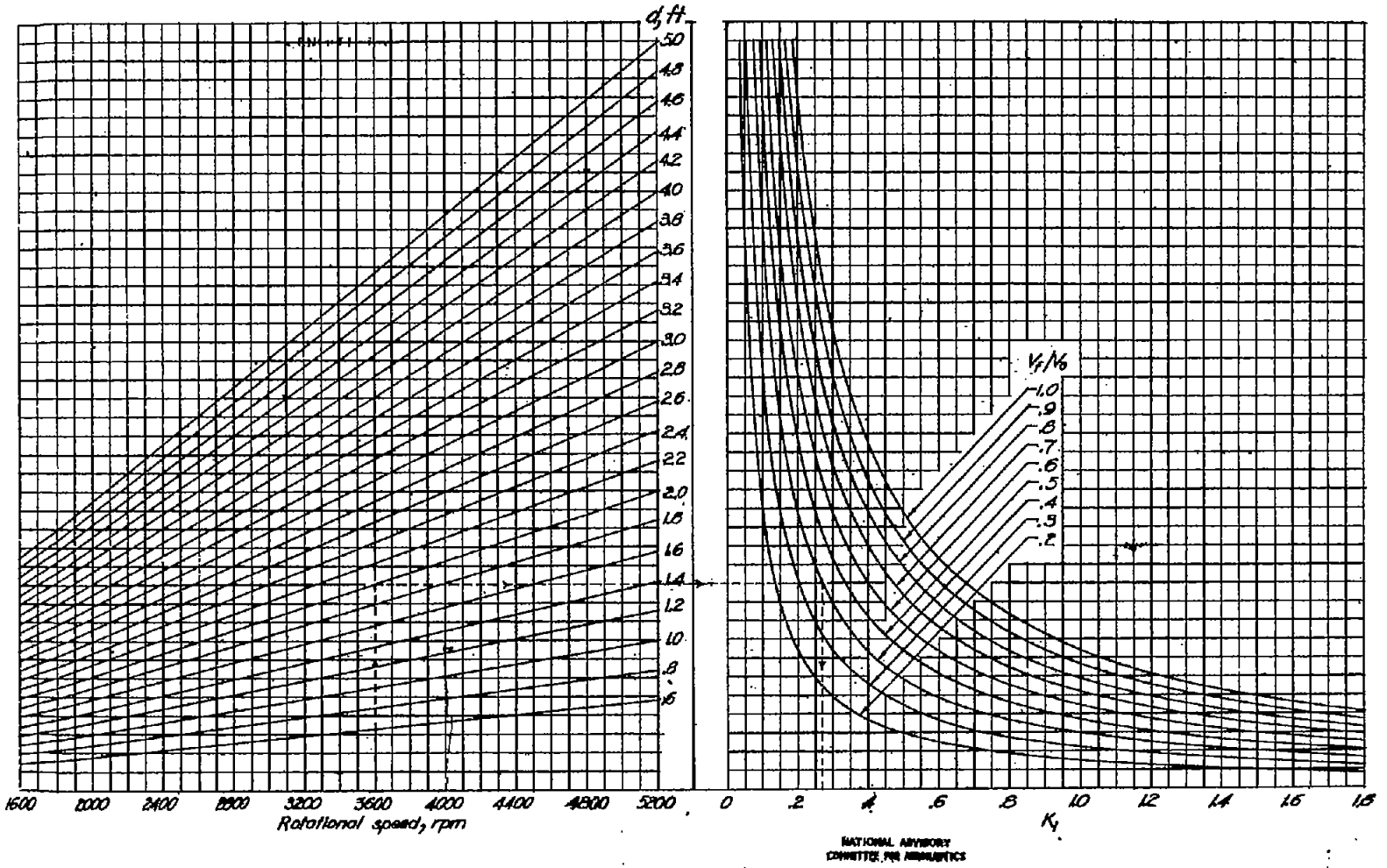

(b) High rotational speed.

Figure 16.- Concluded.

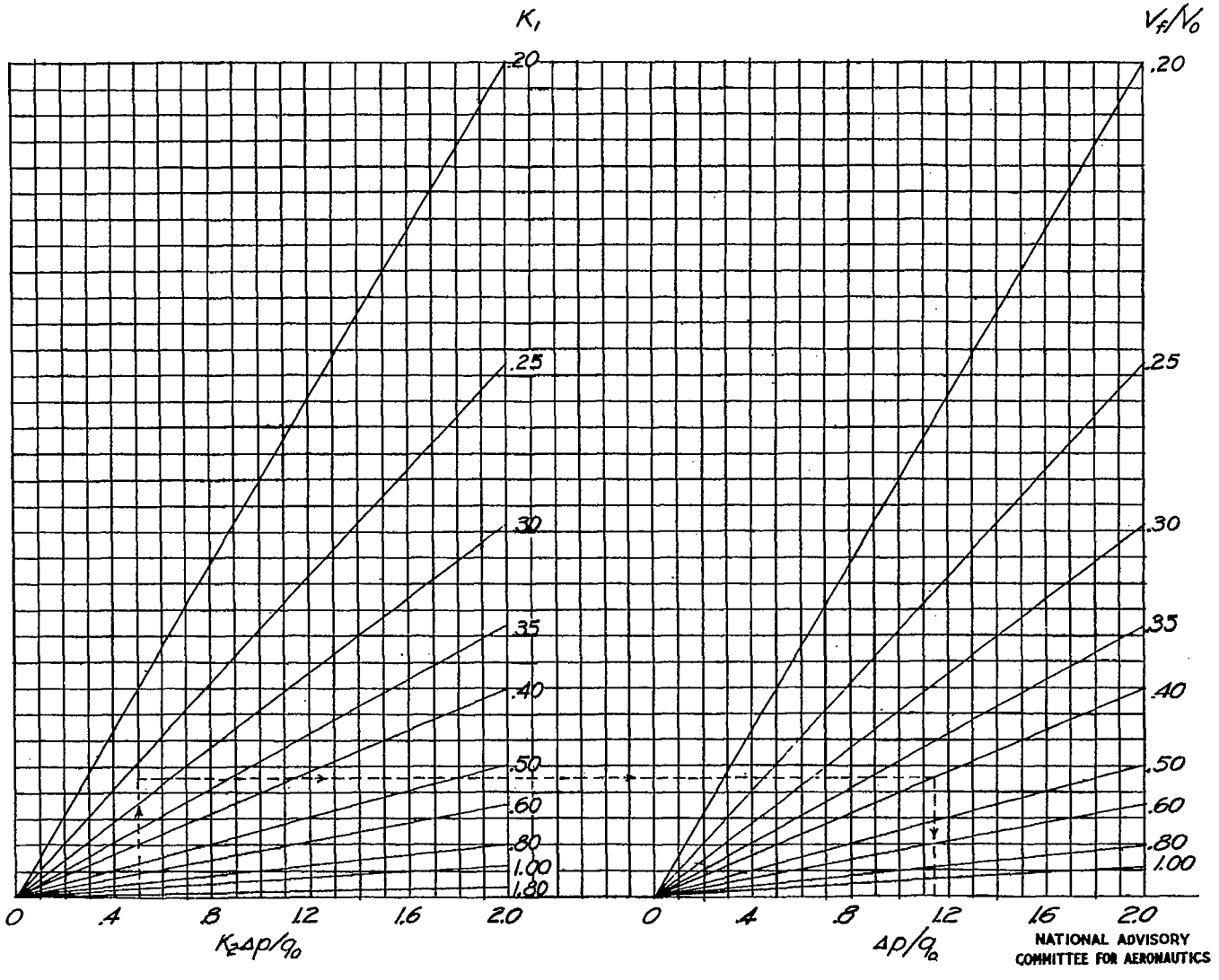

(a) Low pressure rise.

Figure 17.- Charts for determining $\Delta p/q_0$ from $K_2\Delta p/q_0$.

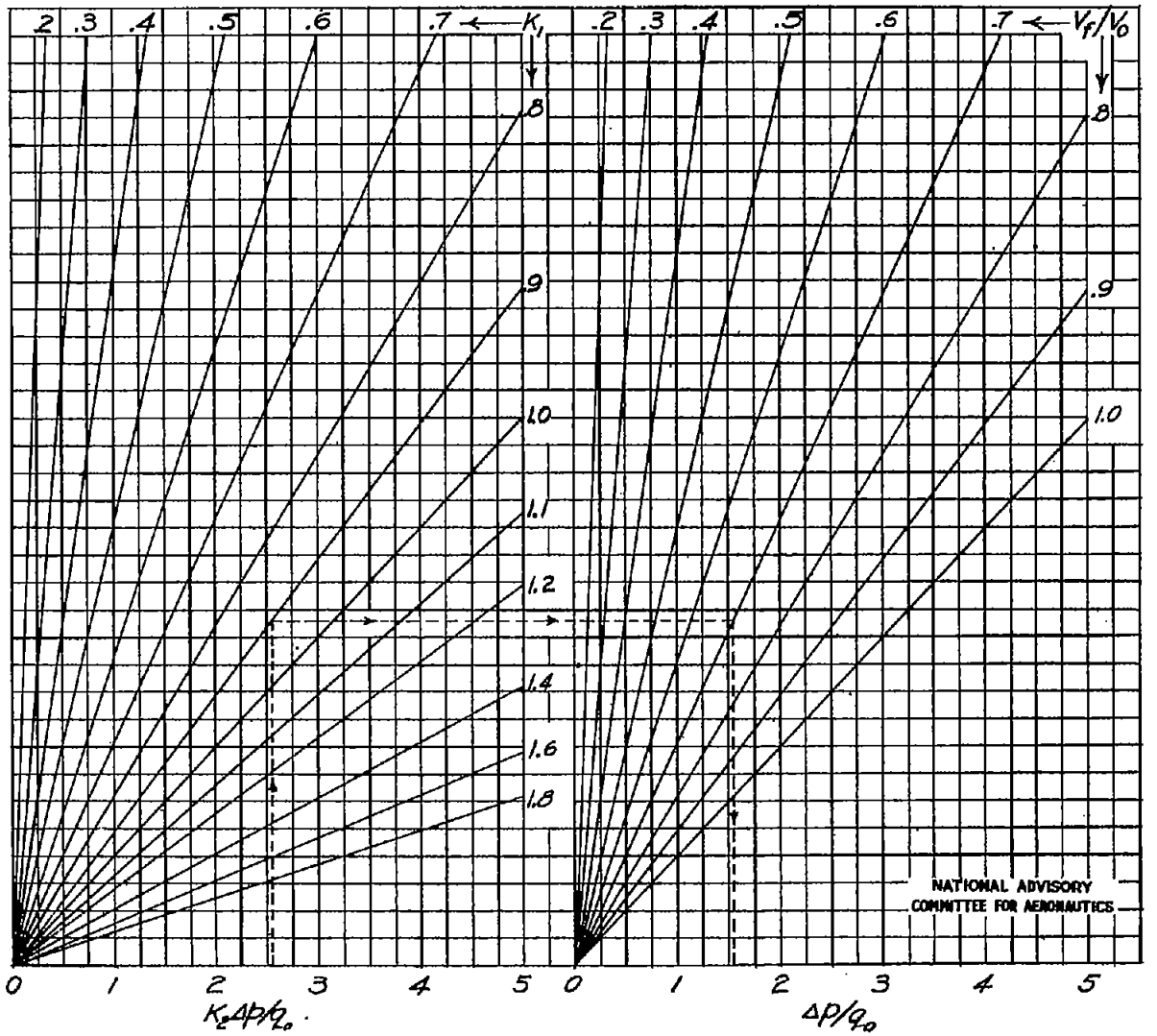

(b) High pressure rise.

Figure 17.- Concluded.

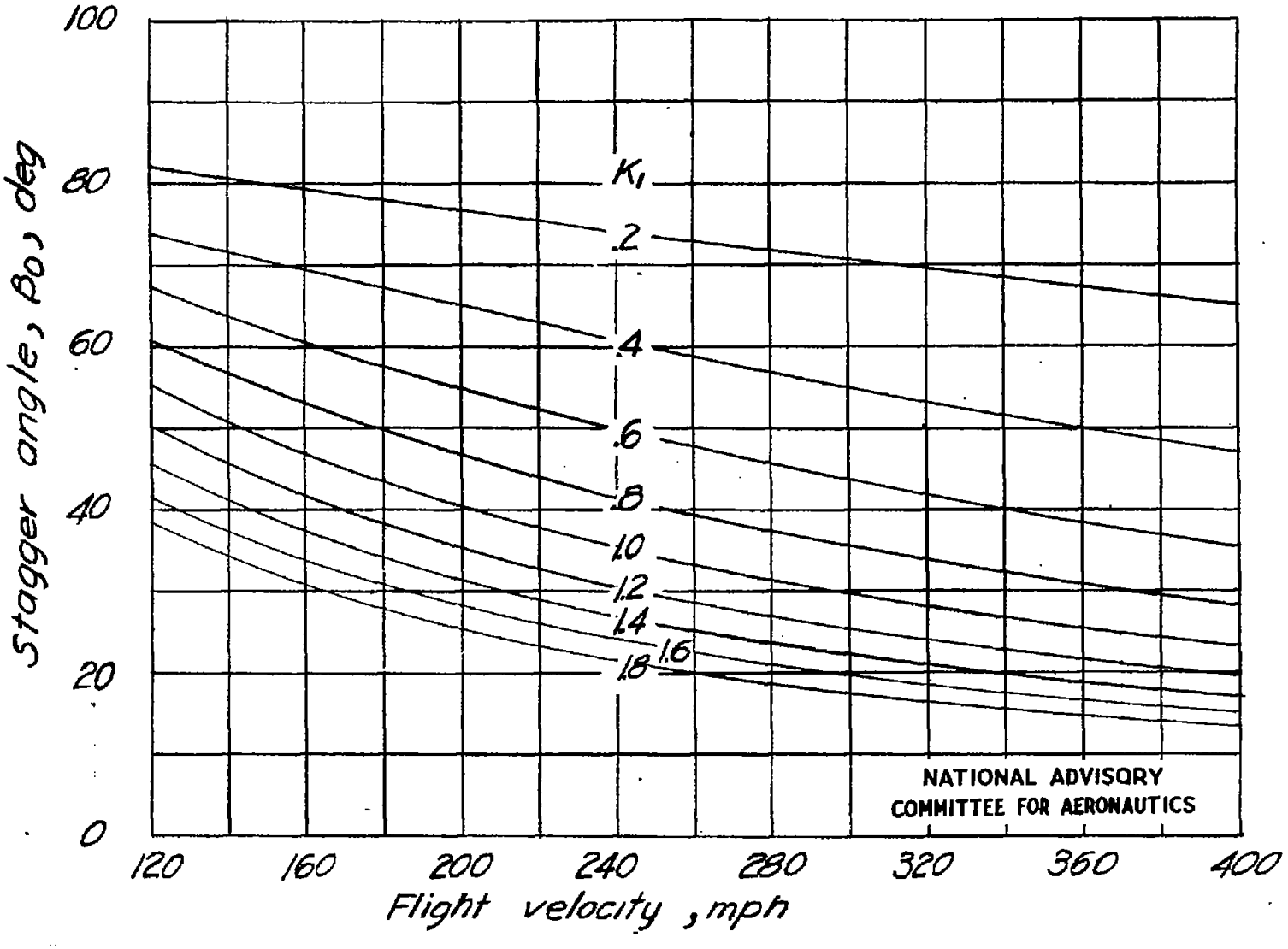

Figure 18.- Variation of β_0 with K_1 and flight velocity for rotor-stator and rotor.

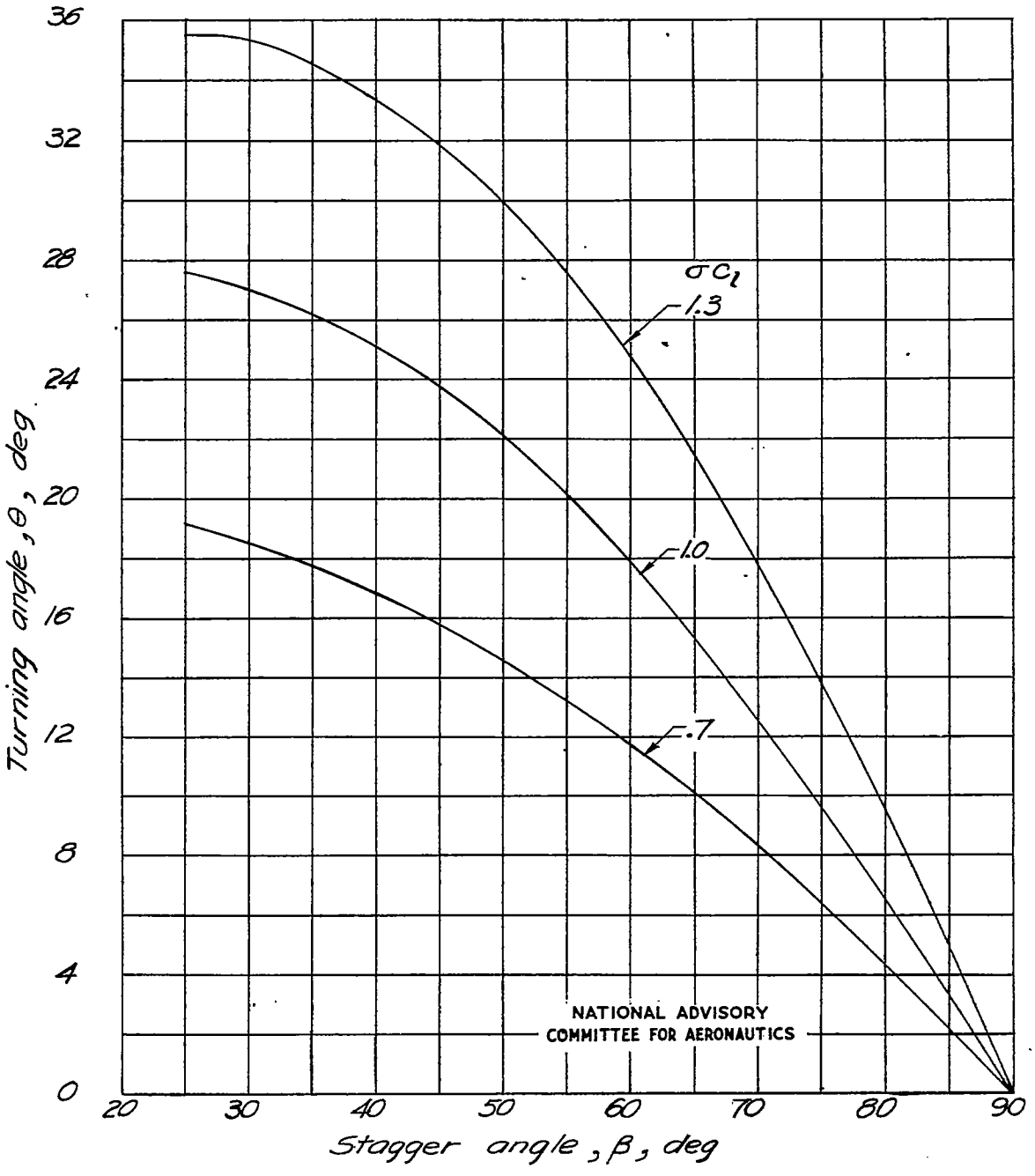

Figure 19.- Variation of turning angle with stagger angle for σc_l = 0.7, 1.0, and 1.3.